one of the RhoGEF/DH proteins that interact with and activate these Rho/Rac molecules leading to actin re-arrangement during phagocytosis. Truncated EhFP4 lacking the FYVE domain and CT domain also weakly bound to three additional Rho/Rac: RacA, 140.m00084 and 69.m00185 (K. Nakada-Tsukui, unpublished), which may indicate that the substrate specificity is also attributable in part to the FYVE as well as the RhoGEF/DH domain.

To date three Dbl family RhoGEF molecules were characterized from *E. histolytica* (Aguilar-Rojas *et al.*, 2005; Arias-Romero *et al.*, 2007; Gonzalez De la Rosa *et al.*, 2007). It has been shown that EhGEF1 and EhGEF2 activate EhRacG, while EhGEF3 activates EhRacA and EhRho1 *in vitro*. EhRacA, EhRacG and EhGEF2 were previously shown to be involved in erythrophagocytosis (Ghosh and Samuelson, 1997; Guillen *et al.*, 1998; Marion *et al.*, 2005; Gonzalez De la Rosa *et al.*, 2007). Thus, the lack of interaction of EhFP4 with EhRacA and EhRacG may indicate that *E. histolytica* possesses multiple signalling pathways regulated by RhoGEFs leading to cytoskeletal re-arrangement during phagocytosis.

Among other proteins shown to be involved in phagocytosis, i.e. p21 activated kinase PAK, and calcium binding protein EhCaBP1 (Labruyere *et al.*, 2003; Jain *et al.*, 2008), we showed partial colocalization of EhCaBP1 and EhFP4. EhCaBP1 associated with the phagocytic cup only for 12 s in the very early phase of phagocytosis (Jain *et al.*, 2008). Together with the restricted colocalization of EhFP4 and EhCaBP1 at the proximal region of the phagocytic cup, these data suggest major differences in the localization and kinetics between EhFP4 and EhCaBP1. Although we were not able to monitor the kinetics of EhFP4 recruitment to the phagocytic cup in a time-lapse imaging in this study, the fact that EhFP4 was also found at the distal region of the phagocytic cups suggests that the dissociation of EhCaBP1 from the phagocytic cup precedes that of EhFP4.

Differential effects of the FYVE domain from amoebic EhFP4 and mammalian Hrs on CHO cell phagocytosis

As shown in Fig. 6, overexpression of EhFP4-FYVE repressed CHO cell phagocytosis while Hrs–FYVE enhanced it. While the inhibitory effect by EhFP4-FYVE can be explained as a competition with endogenous EhFP4, the positive effect of Hrs–FYVE on phagocytosis appears to be puzzling. It has been shown that expression of GFP fused with FYVE domain causes enlargement of endosomes (Gillooly *et al.*, 2000; Chuang *et al.*, 2007). Expression of the FYVE domain dissociates endogenous SARA (Smad anchor for receptor activation) from the rhodopsin-laden vesicles and elicits a dominant negative effect on the phospholipid-directed vesicular trafficking of rhodopsin to the outer segment, light-sensing organelle, of the vertebrate rod photoreceptor (Chuang *et al.*, 2007). These reports suggest that overexpression of FYVE domain caused dominant negative effect on PtdIns(3)P signalling. It has also been shown that inhibition of PtdIns(3)P production by wortmannin repressed RBC phagocytosis and endocytosis in *E. histolytica* (Ghosh and Samuelson, 1997). Thus, our finding that expression of GFP–Hrs–FYVE enhanced CHO cell phagocytosis in *E. histolytica* was unexpected.

There are a few possible explanations for the enhancement of CHO cell phagocytosis by Hrs–FYVE. First, GFP–Hrs–FYVE may immobilize PtdIns(3)P on the site of internalization (the phagocytic cup), and constitutively activate downstream Rho/Rac effectors via recruitment of unidentified EhFP. Second, GFP–Hrs–FYVE may perturb normal PtdIns(3)P metabolism, e.g. by inhibiting dephosphorylation of PtdIns(3)P, which results in accumulation of PtdIns(3)P. Although our finding of the enhancement of phagocytosis by GFP–Hrs–FYVE appears to contradict with the previous study where RBC phagocytosis and endocytosis were inhibited by wortmannin (Ghosh and Samuelson, 1997), the negative effects of wortmannin on phagocytosis could be attributable to other PtdIns signalling cascades because wortmannin is known to affect not only type III PI3K but also other kinds of lipid kinases (Wymann and Pirola, 1998; Oude Weernink *et al.*, 2004).

Opposite effects of the Hrs–FYVE domain on bead and CHO cell phagocytosis

While expression of GFP–Hrs–FYVE enhanced CHO cell phagocytosis (Fig. 6), it repressed phagocytosis of carboxylated beads. This observation clearly indicates that molecular mechanisms of phagocytosis of mammalian cells and negatively charged beads are different. Marion *et al.* (2005) reported remarkable differences in the protein profiles between phagosomes isolated using non-coated latex beads and those with human serum-coated beads. Taken together, these data suggest that PtdIns signals and pathways for phagocytosis are differentially triggered and transduced depending on targets to be ingested. We often observed that an *E. histolytica* trophozoite adhered to CHO cells but not internalize them. Such a trophozoite often appears to start internalization when initiated by contact with another amoeba trophozoite (K. Nakada-Tsukui, unpublished). However, we have not yet identified the signals from the neighbouring trophozoite that trigger internalization.

Finally, discovery and characterization of the unique molecular mechanisms of phagocytosis in parasitic protists should shed light on the evolution of this biological process, which is conserved from free-living and parasitic protists to professional phagocytes in higher eukaryotes.

Experimental procedures

Cells and reagents

Trophozoites of *E. histolytica* strain HM-1:IMSS cl6 (Diamond *et al.*, 1972) were maintained axenically in Diamond's BI-S-33 medium (Diamond *et al.*, 1978) at 35.5°C. Amoeba transformants were cultured in the presence of 10 or 40 μg ml^{-1} Geneticin (Invitrogen, San Diego, CA). Chinese hamster ovary cell lines (CHO) were maintained in F12 medium (Invitrogen, San Diego, CA) supplied with 10% fetal calf serum (MBL, Nagoya, Japan) at 37°C with 5% CO_2. Promastigotes of GFP-expressing *Leishmania amazonensis* (Chan *et al.*, 2003), a gift from Dr K. P. Chang, Rosalind Franklin University, and Dr S. Kawazu, OUAVM, were cultured in 199 medium (Nissui Pharmaceutical, Tokyo, Japan) supplemented with 10% heat-inactivated fetal calf serum, 25 mM Hepes and 5 mg ml^{-1} tunicamycin at 26°C. *Escherichia coli* strain DH5α was purchased from Life Technologies (Tokyo, Japan). All chemicals of analytical grade were purchased from Sigma-Aldrich (Tokyo, Japan) unless otherwise stated.

Plasmid construction

Standard techniques were used for routine DNA manipulation, subcloning and plasmid construction as previously described (Sambrook, 2001). To produce recombinant full-length or partial proteins of EhFP4, a full-length EhFP4, a region containing DH and PH domains (aa 1–333), or a region containing DH domain only (aa 1–266) was PCR-amplified and subcloned into pColdTF vector (Takara, Tokyo Japan) and expressed as Histidine tag-trigger factor (TF)-fused recombinant protein (TF–EhFP4FL, TF–EhFP4DH–PH or TF–EhFP4–DH respectively). Two EhFP4 full-length variants containing two or one mutation, His365Ser/His366Ser (HS) and Cys375Ser (CS) mutants, were generated by PCR-based site-directed mutagenesis. Addition of TF significantly improved solubility of both full-length and truncated forms of recombinant EhFP4. Since we failed to generate soluble GST-fused full-length EhFP4, TF-fused recombinant protein was used in the binding experiments. To produce GST-fused small GTPases, the open reading frames of 108.m00133 (EhRacC; Lohia and Samuelson, 1993), 52.m00167 (EhRho1; Lohia and Samuelson, 1996), 140.m00084, 146.m00106 (EhRacG; Guillen *et al.*, 1998), 16.m00303 (EhRacD; Lohia and Samuelson, 1993), 197.m00080 (EhRacA; Lohia and Samuelson, 1993), 296.m00051, 87.m00159, 46.m00231 and 69.m00185 were PCR-amplified and subcloned into pGEX6p-2 vector (GE Healthcare UK, Buckinghamshire, UK). GST–EhRab7A was prepared as previously described (Nozaki *et al.*, 1998). To produce GST-fused partial EhFP4 proteins, FYVE or carboxyl-terminal (CT) domain (aa 321–422 and 407–495, respectively) was PCR-amplified and subcloned into pGEX6p-2.

We constructed vectors to express either a protein with three tandem copies of the influenza virus haemagglutinin (HA) epitopes at the amino terminus, or a fusion protein with three tandem copies of the c-myc (Myc) epitope followed by RFP at the amino terminus. These plasmids were designated as pEhExHA and pKT-MR respectively. The pEhExHA vector was generated by the insertion of annealed oligonucleotides corresponding to three tandem copies of the HA epitope flanked by 5′ BglII site and 3′ SmaI and XhoI sites into the BglII-XhoI site of pEhEx (Nozaki *et al.*, 1998). RFP protein coding region was PCR-amplified using pRSETB-mRFP, a gift from Dr A. Miyawaki, Riken, as a template, with SmaI and XhoI restriction sites, and subcloned into pKT-M (Saito-Nakano *et al.*, 2004) to generate pKT-MR. To develop amoeba lines expressing Myc-GFP or Myc-RFP fused with two tandem copies of the FYVE domain of Hrs, plasmids were constructed by inserting a fragment containing the Hrs-2xFYVE PCR-amplified from pEGFP-2xFYVE, a gift from Dr Tamotsu Yoshimori, Osaka Univ., into pKT-MG and pKT-MR, to generate pKT-MG-Hrs–FYVE and pKT-MR-Hrs–FYVE respectively. The same fragment was used to generate a plasmid for expressing GST-fused Hrs-2xFYVE recombinant protein by inserting the fragment into to the pGEX6p-2 vector (pGEX6p-2-Hrs–FYVE). The FYVE domain of EhFP4 (aa 333–407) was PCR-amplified and two tandem copies of the domain were subcloned into pKT-MG to produce pKT-MG-EhFP4-FYVE. To generate a vector that would express HA-EhFP fusion proteins in the amoeba, the protein coding regions of EhFP1, 2, 4 and 5 were amplified from an *E. histolytica* cDNA library using appropriate primers, designed based on nucleotide sequences found in the *E. histolytica* genome database (http://www.tigr.org/tdb/e2k1/eha1), with recognition sites for restriction enzymes. The PCR products were cloned into SmaI-XhoI site of pEhExHA vector and were designated as pEhExHA-EhFP1, 2, 3 and 5 respectively.

Amoeba transformation

Plasmids were introduced into the amoeba trophozoites by lipofection as previously described (Nozaki *et al.*, 1999). Geneticin (G418) was added, 24 h after transfection, at a concentration of 1 μg ml^{-1}, and increased gradually for approximately 2 weeks until the drug concentration reached 40 μg ml^{-1} for the pKT-MG, pKT-MG-Hrs–FYVE, pKT-MG-EhFP4-FYVE, pKT-MR and pKT-MR-Hrs–FYVE transformants, and 10 μg ml^{-1} for the pEhExHA-EhFP transformants.

Assays for EhFP4-Rho/Rac binding and Rho guanine nucleotide exchange activity

Approximately 15 μg of GST–Rho/Rac, GST–Rab7A or GST recombinant protein was mixed with 20 μl of glutathione-Sepharose resin (50% suspension), and incubated at 4°C on a rocking platform for 2 h. After the GST–Rho/Rac-bound resin was incubated with EDTA buffer (10 mM EDTA, 20 mM Hepes pH 7.5, 100 mM NaCl and 1 mM DTT) to remove guanine nucleotides, the resin was incubated with 15 μg of TF–EhFP4FL, TF–EhFP4DH–PH or TF in binding buffer (50 mM Hepes pH 7.5, 10 mM MgCl2, 1 mM EDTA, 1 mM DTT, and 0.05% Triton X-100) at 4°C for 16 h. Unbound proteins ('unbound') were collected, and the resin washed extensively with binding buffer. The bound proteins were dissociated from the resin by adding SDS-PAGE sample buffer ('pull-down'). The 'unbound' and 'pull down' fractions were subjected to SDS-PAGE and immunoblot with anti-His monoclonal antibody (Cell Signaling Technology, Danvers, MA, USA) or anti-GST polyclonal antibody (GE healthcare UK). The membranes were washed, and then incubated with alkaline phosphate-conjugated anti-mouse IgG (Cell Signaling Technology) or anti-rabbit IgG (Jackson Laboratory, Main, USA) for 1 h. Proteins were visualized by AP Conjugate Substrate Kit (Bio-Rad, Hercules, CA, USA).

RhoGEF activities of the EhFP4FL, EhFP4 DH-PH, EhFP4 DH, EhFP4FL HS and EhFP4FL CH mutants were determined

by using RhoGEF exchange assay biochem kit (BK100; cytoskeleton, Denver, CO) and human Rac1(hRac1), hCdc42, hRhoA and 146.m00106 (EhRacG), 16.m00303 (EhRacD), 140.m00084, 296.m00051, 87.m00159, 46.m00231 and 69.m00185.

Live cell imaging

Approximately 5×10^5 cells of *E. histolytica* GFP–Hrs–FYVE transformants were cultured on a 35 mm collagen-coated glass-bottom culture dish (MatTek Corporation, Ashland, MA) in 3 ml of BI-S-33 medium under anaerobic conditions. CHO cells were stained for 30 min with 20 μM Cell tracker blue dye or Cell tracker orange dye (Molecular probes, Eugene, OR) in F12 medium containing 10% FCS. After staining, CHO cells were washed three times with fresh BI-S-33 medium, and approximately 2×10^5 CHO cells in 200 μl BI-S-33 medium were added to the GFP–Hrs–FYVE expressing amoeba in a glass-bottom dish. The culture was carefully covered with a coverslip, and overloaded medium was removed. The junction of the coverslip and slide glass was sealed with nail polish, and the culture was incubated at 35°C in a temperature control unit on an AS Multi Dimension Workstation (AS-MDW, Leica Microsystems, Wetzlar, Germany) equipped with a 63×/NA 1.30 oil immersion objective and CCD camera (Coolsnap HQ, Roper Scientific, Duluth, GA). Fluorescence images of 59 continuous slices (z-stack) with 0.5 μm intervals were obtained every 20 s with the BGR filter at excitation wavelengths 492.3 nm for GFP and 389.9 nm for Cell tracker blue.

For confocal microscopic analysis, the culture was incubated at 38°C on the heating insert of Zeiss LSM510 META (Carl-Zeiss microimaging, Jena, Germany) equipped with a 63×/NA 1.4 oil immersing objective with a piezo controller. GFP was excited with the 488 nm laser line of an argon laser with a 505–530 nm filter for emission. Cell tracker orange was excited with the 543-nm line of a HeNe laser, with a 560-nm long pass filter for emission. In Video S1, images were taken every 1 s, while in Video S2, images of 11 slices with 2 μm intervals were obtained every 10 s. The profile of GFP–Hrs–FYVE signal on a nascent phagosome, shown in Video S1, was analysed using the *profile tool* in the LSM software.

*Measurement of phagosome pH and degradation of GFP–*L. amazonensis

Phagosome pH and degradation of GFP–*L. amazonensis* in RFP and RFP-FYVE-overexpressing *E. histolytica* transformants were measured as previously described (Mitra *et al.*, 2005).

Production of Anti-EhFP4 antibody

Anti-EhFP4 antiserum was generated by immunizing two guinea pigs with TF-EhFP4 FL recombinant protein at Kitayama Rabes, Nagano, Japan.

Indirect immunofluorescence assay

Indirect immunofluorescence assay was performed as previously described (Saito-Nakano *et al.*, 2004) with some modifications. Briefly, amoeba transformant cells expressing GFP–Hrs–FYVE, GFP–EhFP4–FYVE, HA-EhFP1, 2, 4 or 5 were harvested and transferred to 8 mm round wells on a slide glass. CHO cells were prestained with 10 μM of Cell tracker orange or 20 μM of Cell tracker green (Molecular Probes, Eugene, OR) for 30 min, harvested, and washed with BI-S-33 medium. Approximately 1.5×10^5 amoebae were incubated with 1.5×10^5 of Cell tracker-stained CHO cells for the times indicated, and after washing, fixed with 3.7% paraformaldehyde in phosphate buffered saline (PBS), pH 7.2 for 10 min. The amoebae and CHO cells were washed and then permeabilized with 0.2% saponin in PBS containing 1% BSA for 10 min, and reacted with a primary antibody diluted at 1:1000 (anti-HA monoclonal antibody, 11MO, Covance, Princeton, NJ), 1:500 (anti-EhFP4 antiserum), or 1:100 (anti-EhCaBP1 antiserum) in PBS containing 0.2% saponin and 1% BSA. After washing, the samples were then incubated with Alexa Fluor 488-, 568- or 633- conjugated anti-rabbit, anti-mouse, or anti-guinea pig secondary antibody (1:1000) for 1 h. For phallacidin staining, fixed and permeabilized trophozoites were incubated with 0.33 μM of BODIPY FL phallacidin (Molecular Probes, Eugine, OR) for 20 min. The samples were examined on a Carl-Zeiss LSM 510 META confocal laser-scanning microscope, and images were analysed using LSM510 software.

DNA microarray

A custom short oligonucleotide microarray was fabricated by Virginia Bioinformatics Institute, Blacksburg, VA with a license from Affymetrix (Santa Clara, CA, USA) as previously described (Gilchrist *et al.*, 2006). These arrays were designed with probes targeting both predicted mRNAs (9435 of the 9938 predicted genes) and intergenic regions. Total RNA from three independent cultures, isolated as previously described (Gilchrist *et al.*, 2006), were used to generate expression profiles, which showed a correlation coefficient greater than 0.95, indicating that the result was reproducible. Data were further analysed with the GCOS software (Affymetrix, Santa Clara, CA, USA). Detailed analysis of the microarray data will be presented elsewhere.

Phosphoinositide binding assay

Nitrocellulose membranes with spotted various phosphoinositides and other lipids (PIP strips) were purchased from Echelon Research Laboratories (Salt Lake City, UT). Membranes were blocked with 1% skim-milk in PBS for 1 h at room temperature. Blocked membranes were incubated overnight at 4°C with 10 μg ml^{-1} TF, TF–EhFP4FL, TF-EhFP4 DH-PH, TF-EhFP4 DH, TF–EhFP4FL HS and TF–EhFP4FL CS mutants, and recombinant proteins GST–EhFP4–FYVE and GST–EhFP4–CT. The membranes were then washed three times for 10 min in PBS containing 0.1% tween-20. The membranes were incubated with anti-His monoclonal antibody (1:500 dilution, Cell Signaling Technology) or anti-GST polyclonal antibody (1:500 dilution, GE healthcare UK), for 1 h at room temperature followed by washing. The membranes were incubated with HRP-conjugated anti-mouse secondary antibody (1:500 dilution) or alkaline phosphatase (AP)-conjugated anti-goat secondary antibody (1:1000 dilution) for 1 h at room temperature. After washing, the proteins were detected by chemiluminescence as described above (for HRP-conjugated secondary antibody) or with an AP conjugate substrate kit (Bio-Rad, Hercules, CA) (for AP-conjugated secondary antibody).

Phagocytosis assay

Approximately 10^5 amoebae were grown overnight in a 24-well plate under anaerobic conditions. Roughly $4–8 \times 10^5$ of Cell tracker orange-loaded CHO cells or 5 μl of Nile Red fluorescent carboxylate-modified FluoSphere microspheres (Molecular Probes, Eugene, OR) was added to the amoeba, and incubated for 0, 10, 30 or 60 min. After incubation, the amoebae were washed once with warm PBS containing 250 mM galactose (PBS-galactose), and 450 μl of PBS-galactose was added. The plate was chilled on ice and detached amoebae were recovered and analysed by two-colour flow cytometry (FACSCalibur, BD, Franklin Lakes, NJ).

Accession numbers

The nucleotide sequence data reported in this paper are available in the DDBJ/GenBank/EBI databases with the following accession numbers: EhFP1, XP_651719; EhFP2, XP_655361; EhFP3, XP_650743; EhFP4, XP_656365; EhFP5, XP_649382; EhFP6, XP_651964; EhFP7, XP_654401; EhFP8, XP_651711; EhFP9, XP_656765; EhFP10, XP_651436;EhFP11, XP_651674; EhFP12, XP_656065; 108.m00133, EHI_070730, XP_652693; 52.m00167, EHI_029020, XP_654488; 140.m00084, XP_651936; 146.m00106, EHI_129750, XP_651800; 16.m00303, EHI_012240, XP_656184; 197.m00080, EHI_197840, XP_650831; 296.m00051, EHI_135450, XP_649502; 87.m00159, EHI_146180, XP_653308; 46.m00231, EHI_194390, XP_654700; 69.m00185, EHI_192450, XP_653885

Acknowledgements

We thank Alok Bhattacharya, Jawaharal Nehru University, for EhCaBP1 antibody, Miguel Vargas, CINVESTAV, for EhGEF1 and EhRacG construct, Gil Penuliar for proof reading the manuscript, Yoko Yamada, Tomoko Akuzawa, Atsushi Furukawa, Mai Nudejima, Fumie Tokumaru, and Yasuo Shigeta for technical assistance. This work was supported by the Grant-in-Aid for Scientific Research from the Ministry of Education, Culture, Sports, Science and Technology of Japan awarded to T.N. (18050006, 18073001, 18GS0314, 20390119) and K.N.T. (18790291, 20790323), a grant for Research on Emerging and Re-emerging Infectious Diseases from the Ministry of Health, Labour, and Welfare (H20-Shinkosaiko-Ippan-016), and a grant for research to promote the development of anti-AIDS pharmaceuticals from the Japan Health Sciences Foundation awarded to T.N.

References

Ackers, J.P., and Mirelman, D. (2006) Progress in research on *Entamoeba histolytica* pathogenesis. *Curr Opin Microbiol* **9:** 367–373.

Aguilar-Rojas, A., de Jesus Almaraz-Barrera, M., Krzeminski, M., Robles-Flores, M., Hernandez-Rivas, R., Guillen, N., *et al.* (2005) *Entamoeba histolytica*: inhibition of cellular functions by overespression of EhGEF1, a novel Rho/Rac guanine nucleotide exchange factor. *Exp Parasitol* **109:** 150–162.

Arias-Romero, L.E., de Jesus Almaraz-Barrera, M., Diaz-Valencia, J.D., Rojo-Dominguez, A., Hernandez-Rivas, R., and Vargas, M. (2006) EhPAK2, a novel p21-activated kinase, is required for collagen invasion and capping in *Entamoeba histolytica*. *Mol Biochem Parasitol* **149:** 17–26.

Arias-Romero, L.E., Gonzalez de la Rosa, C.H., de Jesus Almaraz-Barrera, M., Diaz-Valencia, J.D., Sosa-Peinado, A., and Vargas, M. (2007) EhGEF3, a novel Dbl family member, regulates EhRacA activation during chemotaxis and capping in *Entamoeba histolytica*. *Cell Motil Cytoskeleton* **64:** 390–404.

Balla, T. (2005) Inositol-lipid binding motifs: signal integrators through protein-lipid and protein–protein interactions. *J Cell Sci* **118:** 2093–2104.

Botelho, R.J., Scott, C.C., and Grinstein, S. (2004) Phosphoinositide involvement in phagocytosis and phagosome maturation. *Curr Top Microbiol Immunol* **282:** 1–30.

Burd, C.G., and Emr, S.D. (1998) Phosphatidylinositol (3) -phosphate signaling mediated by specific binding to RING FYVE domains. *Mol Cell* **2:** 157–162.

Chan, M.M., Bulinski, J.C., Chang, K.P., and Fong, D. (2003) A microplate assay for *Leishmania amazonensis* promastigotes expressing multimeric green fluorescent protein. *Parasitol Res* **89:** 266–271.

Chua, J., and Deretic, V. (2004) *Mycobacterium tuberculosis* reprograms waves of phosphatidylinositol 3-phosphate on phagosomal organelles. *J Biol Chem* **279:** 36982–36992.

Chuang, J.Z., Zhao, Y., and Sung, C.H. (2007) SARA-regulated vesicular targeting underlies formation of the light-sensing organelle in mammalian rods. *Cell* **130:** 535–547.

Clark, C.G., Alsmark, U.C., Tazreiter, M., Saito-Nakano, Y., Ali, V., Marion, S., *et al.* (2007) Structure and content of the *Entamoeba histolytica* genome. *Adv Parasitol* **65:** 51–190.

Coudrier, E., Amblard, F., Zimmer, C., Roux, P., Olivo-Marin, J.C., Rigothier, M.C., and Guillen, N. (2005) Myosin II and the Gal-GalNAc lectin play a crucial role in tissue invasion by *Entamoeba histolytica*. *Cell Microbiol* **7:** 19–27.

Crespo, P., Schuebel, K.E., Ostrom, A.A., Gutkind, J.S., and Bustelo, X.R. (1997) Phosphotyrosine-dependent activation of Rac-1 GDP/GTP exchange by the vav proto-oncogene product. *Nature* **385:** 169–172.

Diamond, L.S., Mattern, C.F., and Bartgis, I.L. (1972) Viruses of *Entamoeba histolytica*. I. Identification of transmissible virus-like agents. *J Virol* **9:** 326–341.

Diamond, L.S., Harlow, D.R., and Cunnick, C.C. (1978) A new medium for the axenic cultivation of *Entamoeba histolytica* and other *Entamoeba*. *Trans R Soc Trop Med Hyg* **72:** 431–432.

Ehrenkaufer, G.M., Haque, R., Hackney, J.A., Eichinger, D.J., and Singh, U. (2007) Identification of developmentally regulated genes in *Entamoeba histolytica*: insights into mechanisms of stage conversion in a protozoan parasite. *Cell Microbiol* **9:** 1426–1444.

Ellson, C.D., Anderson, K.E., Morgan, G., Chilvers, E.R., Lipp, P., Stephens, L.R., and Hawkins, P.T. (2001) Phosphatidylinositol 3-phosphate is generated in phagosomal membranes. *Curr Biol* **11:** 1631–1635.

Estrada, L., Caron, E., and Gorski, J.L. (2001) Fgd1, the Cdc42 guanine nucleotide exchange factor responsible for faciogenital dysplasia, is localized to the subcortical actin cytoskeleton and Golgi membrane. *Hum Mol Genet* **10:** 485–495.

Franco-Barraza, J., Zamudio-Meza, H., Franco, E., del Carmen Dominguez-Robles, M., Villegas-Sepulveda, N., and Meza, I. (2006) Rho signaling in *Entamoeba histolytica* modulates actomyosin-dependent activities stimulated during invasive behavior. *Cell Motil Cytoskeleton* **63:** 117–131.

Fratti, R.A., Backer, J.M., Gruenberg, J., Corvera, S., and Deretic, V. (2001) Role of phosphatidylinositol 3-kinase and Rab5 effectors in phagosomal biogenesis and mycobacterial phagosome maturation arrest. *J Cell Biol* **154:** 631–644.

Frederick, J.R., and Petri, W.A., Jr (2005) Roles for the galactose-/N-acetylgalactosamine-binding lectin of *Entamoeba* in parasite virulence and differentiation. *Glycobiology* **15:** 53R–59R.

Gaullier, J.M., Simonsen, A., D'Arrigo, A., Bremnes, B., Stenmark, H., and Aasland, R. (1998) FYVE fingers bind PtdIns(3)P. *Nature* **394:** 432–433.

Ghosh, S.K., and Samuelson, J. (1997) Involvement of p21racA, phosphoinositide 3-kinase, and vacuolar ATPase in phagocytosis of bacteria and erythrocytes by *Entamoeba histolytica*: suggestive evidence for coincidental evolution of amebic invasiveness. *Infect Immun* **65:** 4243–4249.

Gilchrist, C.A., Houpt, E., Trapaidze, N., Fei, Z., Crasta, O., Asgharpour, A., *et al.* (2006) Impact of intestinal colonization and invasion on the *Entamoeba histolytica* transcriptome. *Mol Biochem Parasitol* **147:** 163–176.

Gillooly, D.J., Morrow, I.C., Lindsay, M., Gould, R., Bryant, N.J., Gaullier, J.M., *et al.* (2000) Localization of phosphatidylinositol 3-phosphate in yeast and mammalian cells. *EMBO J* **19:** 4577–4588.

Gillooly, D.J., Simonsen, A., and Stenmark, H. (2001) Cellular functions of phosphatidylinositol 3-phosphate and FYVE domain proteins. *Biochem J* **355:** 249–258.

Gonzalez De la Rosa, C.H., Arias-Romero, L.E., de Jesus Almaraz-Barrera, M., Hernandez-Rivas, R., Sosa-Peinado, A., Rojo-Dominguez, A., *et al.* (2007) *Eh*GEF2, a Dbl-RhoGEF from *Entamoeba histolytica* has atypical biochemical properties and participates in essential cellular process. *Mol Biochem Parasitol* **151:** 70–80.

Guillen, N., Boquet, P., and Sansonetti, P. (1998) The small GTP-binding protein RacG regulates uroid formation in the protozoan parasite *Entamoeba histolytica*. *J Cell Sci* **111** (Pt 12): 1729–1739.

Halet, G. (2005) Imaging phosphoinositide dynamics using GFP-tagged protein domains. *Biol Cell* **97:** 501–518.

Haque, R., Mondal, D., Kirkpatrick, B.D., Akther, S., Farr, B.M., Sack, R.B., and Petri, W.A., Jr (2003) Epidemiologic and clinical characteristics of acute diarrhea with emphasis on *Entamoeba histolytica* infections in preschool children in an urban slum of Dhaka, Bangladesh. *Am J Trop Med Hyg* **69:** 398–405.

Huber, C., Mårtensson, A., Bokoch, G.M., Nemazee, D., and Gavin, A.L. (2008) FGD2, a CDC42-specific exchange factor expressed by antigen-presenting cells, localizes to early endosomes and active membrane ruffles. *J Biol Chem* **283:** 34002–34012.

Jain, R., Santi-Rocca, J., Padhan, N., Bhattacharya, S., Guillen, N., and Battacharya, A. (2008) Calcium-binding protein 1 of *Entamoeba histolytica* transiently associates with phagocytic cups in a calcium-independent manner. *Cell Microbiol* **10:** 1373–1389.

Komada, M., Masaki, R., Yamamoto, A., and Kitamura, N. (1997) Hrs, a tyrosine kinase substrate with a conserved double zinc finger domain, is localized to the cytoplasmic surface of early endosomes. *J Biol Chem* **272:** 20538–20544.

Labruyere, E., and Guillen, N. (2006) Host tissue invasion by *Entamoeba histolytica* is powered by motility and phagocytosis. *Arch Med Res* **37:** 253–258.

Labruyere, E., Zimmer, C., Galy, V., Olivo-Marin, J.C., and Guillen, N. (2003) EhPAK, a member of the p21-activated kinase family, is involved in the control of *Entamoeba histolytica* migration and phagocytosis. *J Cell Sci* **116:** 61–71.

Lejeune, A., and Gicquaud, C. (1987) Evidence for two mechanisms of human erythrocyte endocytosis by *Entamoeba histolytica*-like amoebae (Laredo strain). *Biol Cell* **59:** 239–245.

Lejeune, A., and Gicquaud, C. (1992) Target cell deformability determines the type of phagocytic mechanism used by *Entamoeba histolytica*-like, Laredo strain. *Biol Cell* **74:** 211–216.

Lindmo, K., and Stenmark, H. (2006) Regulation of membrane traffic by phosphoinositide 3-kinases. *J Cell Sci* **119:** 605–614.

Loftus, B., Anderson, I., Davies, R., Alsmark, U.C., Samuelson, J., Amedeo, P., *et al.* (2005) The genome of the protist parasite *Entamoeba histolytica*. *Nature* **433:** 865–868.

Lohia, A., and Samuelson, J. (1993) Molecular cloning of a rho family gene of *Entamoeba histolytica*. *Mol Biochem Parasitol* **58:** 177–180.

Lohia, A., and Samuelson, J. (1996) Heterogeneity of *Entamoeba histolytica* rac genes encoding p21rac homologues. *Gene* **173:** 205–208.

Marion, S., Laurent, C., and Guillen, N. (2005) Signalization and cytoskeleton activity through myosin IB during the early steps of phagocytosis in *Entamoeba histolytica*: a proteomic approach. *Cell Microbiol* **7:** 1504–1518.

Mitra, B.N., Yasuda, T., Kobayashi, S., Saito-Nakano, Y., and Nozaki, T. (2005) Differences in morphology of phagosomes and kinetics of acidification and degradation in phagosomes between the pathogenic *Entamoeba histolytica* and the non-pathogenic *Entamoeba dispar*. *Cell Motil Cytoskeleton* **62:** 84–99.

Mitra, B.N., Kobayashi, S., Saito-Nakano, Y., and Nozaki, T. (2006) *Entamoeba histolytica*: differences in phagosome acidification and degradation between attenuated and virulent strains. *Exp Parasitol* **114:** 57–61.

Nakada-Tsukui, K., Saito-Nakano, Y., Ali, V., and Nozaki, T. (2005) A retromerlike complex is a novel Rab7 effector that is involved in the transport of the virulence factor cysteine protease in the enteric protozoan parasite *Entamoeba histolytica*. *Mol Biol Cell* **16:** 5294–5303.

Nozaki, T., Asai, T., Kobayashi, S., Ikegami, F., Noji, M., Saito, K., and Takeuchi, T. (1998) Molecular cloning and characterization of the genes encoding two isoforms of cysteine synthase in the enteric protozoan parasite *Entamoeba histolytica*. *Mol Biochem Parasitol* **97:** 33–44.

Nozaki, T., Asai, T., Sanchez, L.B., Kobayashi, S., Nakazawa, M., and Takeuchi, T. (1999) Characterization of the gene encoding serine acetyltransferase, a regulated

enzyme of cysteine biosynthesis from the protist parasites *Entamoeba histolytica* and *Entamoeba dispar*. Regulation and possible function of the cysteine biosynthetic pathway in *Entamoeba*. *J Biol Chem* **274:** 32445–32452.

Okada, M., Huston, C.D., Oue, M., Mann, B.J., Petri, W.A. Jr, Kita, K., and Nozaki, T. (2006) Kinetics and strain variation of phagosome proteins of *Entamoeba histolytica* by proteomic analysis. *Mol Biochem Parasitol* **145:** 171–183.

Orrico, A., Galli, L., Falciani, M., Bracci, M., Cavaliere, M.L., Rinaldi, M.M., *et al.* (2000) A mutation in the pleckstrin homology (PH) domain of the FGD1 gene in an Italian family with faciogenital dysplasia (Aarskog–Scott syndrome). *FEBS Lett* **478:** 216–220.

Oude Weernink, P.A., Schmidt, M., and Jakobs, K.H. (2004) Regulation and cellular roles of phosphoinositide 5-kinases. *Eur J Pharmacol* **500:** 87–99.

Pasteris, N.G., Cadle, A., Logie, L.J., Porteous, M.E., Schwartz, C.E., Stevenson, R.E., *et al.* (1994) Isolation and characterization of the faciogenital dysplasia (Aarskog–Scott syndrome) gene: a putative Rho/Rac guanine nucleotide exchange factor. *Cell* **79:** 669–678.

Pasteris, N.G., Nagata, K., Hall, A., and Gorski, J.L. (2000) Isolation, characterization, and mapping of the mouse Fgd3 gene, a new Faciogenital Dysplasia (FGD1; Aarskog Syndrome) gene homologue. *Gene* **242:** 237–247.

Powell, R.R., Welter, B.H., Bowersox, B., Attaway, C., and Temesvari, L.A. (2006) *Entamoeba histolytica*: FYVE -finger domains, phosphatidylinositol 3-phosphate biosensors, associate with phagosomes but not fluid filled endosomes. *Exp Parasitol* **112:** 221–231.

Que, X., and Reed, S.L. (2000) Cysteine proteinases and the pathogenesis of amebiasis. *Clin Microbiol Rev* **13:** 196–206.

Rossman, K.L., Der, C.J., and Sondek, J. (2005) GEF means go: turning on RHO GTPases with guanine nucleotide-exchange factors. *Nat Rev Mol Cell Biol* **6:** 167–180.

Saito-Nakano, Y., Yasuda, T., Nakada-Tsukui, K., Leippe, M., and Nozaki, T. (2004) Rab5-associated vacuoles play a unique role in phagocytosis of the enteric protozoan parasite *Entamoeba histolytica*. *J Biol Chem* **279:** 49497–49507.

Saito-Nakano, Y., Mitra, B.N., Nakada-Tsukui, K., Sato, D., and Nozaki, T. (2007) Two Rab7 isotypes, EhRab7A and EhRab7B, play distinct roles in biogenesis of lysosomes and phagosomes in the enteric protozoan parasite *Entamoeba histolytica*. *Cell Microbiol* **9:** 1796–1808.

Sambrook, J.A.R., and Russell, D.W. (2001) *Molecular Cloning*. Cold Spring Harbor, NY: Cold Spring Harbor Laboratory Press.

Schuebel, K.E., Movilla, N., Rosa, J.L., and Bustelo, X.R. (1998) Phosphorylation-dependent and constitutive activation of Rho proteins by wild-type and oncogenic Vav-2. *EMBO J* **17:** 6608–6621.

Scott, C.C., Dobson, W., Botelho, R.J., Coady-Osberg, N., Chavrier, P., Knecht, D.A., *et al.* (2005) Phosphatidylinositol-4,5-bisphosphate hydrolysis directs actin remodeling during phagocytosis. *J Cell Biol* **169:** 139–149.

Stenmark, H., Aasland, R., Toh, B.-H., and D'Arrigo, A. (1996) Endosomal localization of the autoantigen EEA1 is mediated by a zinc-binding FYVE finger. *J Biol Chem* **271:** 24048–24054.

Stenmark, H., Aasland, R., and Driscoll, P.C. (2002) The phosphatidylinositol 3-phosphate-binding FYVE finger. *FEBS Lett* **513:** 77–84.

Suzuki, N., Nakamura, S., Mano, H., and Kozasa, T. (2003) Galpha 12 activates Rho GTPase through tyrosine-phosphorylated leukemia-associated RhoGEF. *Proc Natl Acad Sci USA* **100:** 733–738.

Swanson, J.A., Johnson, M.T., Beningo, K., Post, P., Mooseker, M., and Araki, N. (1999) A contractile activity that closes phagosomes in macrophages. *J Cell Sci* **112** (Pt 3)**:** 307–316.

Vargas, M., and Gonzalez-de la Rosa, C.H. (2007) Structural and functional organization of the RhoGEF proteins from *Entamoeba hisolytica*. In *Advances in the Immunobiology of Parasitic Diseases*. Terrazes, L.I. (ed.). Kerala: Research Signpost, pp. 339–359.

Vieira, O.V., Harrison, R.E., Scott, C.C., Stenmark, H., Alexander, D., Liu, J., *et al.* (2004) Acquisition of Hrs, an essential component of phagosomal maturation, is impaired by mycobacteria. *Mol Cell Biol* **24:** 4593–4604.

Voigt, H., and Guillen, N. (1999) New insights into the role of the cytoskeleton in phagocytosis of *Entamoeba histolytica*. *Cell Microbiol* **1:** 195–203.

Wymann, M.P., and Pirola, L. (1998) Structure and function of phosphoinositide 3-kinases. *Biochim Biophys Acta* **1436:** 127–150.

Yeung, T., Ozdamar, B., Paroutis, P., and Grinstein, S. (2006) Lipid metabolism and dynamics during phagocytosis. *Curr Opin Cell Biol* **18:** 429–437.

Yu, X., Lu, N., and Zhou, Z. (2008) Phagocytic receptor CED-1 initiates a signaling pathway for degrading engulfed apoptotic cells. *PLoS Biol* **6:** e61.

Supporting information

Additional Supporting Information may be found in the online version of this article:

Fig. S1. Measurement of the fluorescence intensity of GFP–Hrs–FYVE on the nascent phagosome. The distribution of the signal intensity at channel 2 (green, GFP) and channel 3 (red, Cell tracker red) on the dissected plane, indicated by red arrows, were plotted using *profile tool* in the Carl Zeiss LSM510 software at two representative time points (top, 0.2 s; bottom, 165.4 s). The time kinetics of the GFP signal on the nascent phagosome is shown in Fig. 1D. Vertical black arrows indicate the region where the fluorescence signal was measured.

Fig. S2. The percentages of phagosomes (upper panel) and the phagocytic cups (lower panel) associated or not associated with GFP–Hrs–FYVE. *E. histolytica* trophozoites expressing GFP–Hrs–FYVE were co-cultured with Cell tracker blue-loaded CHO cells for 10, 30 and 60 min. The amoebae and CHO cells were fixed and examined by Zeiss LSM510. The percentages of the CHO-containing phagosomes and the phagocytic cups that were positive for GFP–Hrs–FYVE (filled bars), or negative (open bars) at indicated time points are shown. The mean and standard deviation of two independent experiments are shown.

Fig. S3. Localization of endogenous EhFP4. Anti-EhFP4 antibody was raised by immunizing guinea pigs with TF–EhFP4FL recombinant protein.

A–E. Localization of EhFP4 in the HA-EhFP4FL-expressing trophozoite. HA-EhFP4FL-expressing trophozoites were co-cultured with Cell tracker-blue-loaded CHO cells for 30 min, fixed and reacted with anti-HA and anti-EhFP4 antibody. The cells were then reacted with Alexa-568 conjugated anti-mouse IgG and Alexa-488 conjugated anti-guinea pig IgG antibody. Arrows indicate the phagocytic cup.

F–N. Localization of endogenous EhFP4 in HM-1:IMSS cl6. HM-1:IMSS cl6 trophozoites were co-cultured with CHO cells and reacted with anti-EhFP4 antibody. Arrows indicate the phagocytic cup. Bars, 10 μm.

Fig. S4. Localization of wild-type EhFP4 (top) and mutant EhFP4 lacking FYVE and C-term domains (bottom) during CHO cell phagocytosis. Three additional trophozoites expressing HA-tagged wild-type EhFP4 (upper panel) or EhFP4DH-PH (lower panel) are shown. See Fig. 3A for experimental details. Arrows indicate HA-EhFP4 on the tunnel-like structure. Open arrowheads indicate structures not associated with FYVE-deficient HA-EhFP4 mutant. Bars, 10 μm.

Fig. S5. Localization of GFP–Hrs–FYVE during erythrophagocytosis. *E. histolytica* trophozoites expressing GFP–Hrs–FYVE were co-cultured with gerbil erythrocytes for 40 min, fixed and examined by confocal microscopy. Arrows indicate GFP-positive phagosomes. Bars, 10 μm.

Video S1. A GFP–Hrs–FYVE-expressing *E. histolytica* trophozoite ingests a Cell tracker orange-loaded CHO cell (pseudocolored in red). Images were captured every s on Zeiss LSM510 META. An *E. histolytica* trophozoite, which remains at the centre in the course of movie, ingests a CHO cell. Note that this trophozoite has already ingested another CHO cell prior to the beginning of the movie, and thus contains two phagosomes on this plane: one GFP–Hrs–FYVE-positive and one negative phagosome. This trophozoite adheres to a CHO cell (0 min), and initiates internalization (0.082 min). GFP–Hrs–FYVE starts to accumulate on the phagocytic cup (0.824 min). The entire circumference of the enclosed phagosome becomes positive for GFP–Hrs–FYVE (1.483 min). A thread-like structure connecting two phagosomes is also visible (2.801 min). An extended CHO cell being simultaneously internalized by two neighbouring trophozoites, which is typically seen in 'slow phagocytosis', is also visible (e.g. 0 min).

Video S2. This movie shows the kinetics of 'slow phagocytosis'. A GFP–Hrs–FYVE expressing-*E. histolytica* trophozoite ingests a Cell tracker orange-loaded CHO cell. Images of 11 slices with 2 μm intervals were obtained every 10 s on Zeiss LSM510 META. Time series of a single representative plane are shown. A trophozoite adheres to a CHO cell (0.17 min) and starts internalization (0.33 min). The GFP–Hrs–FYVE-positive tunnel structure is visible for at least 5.17 min, supporting the continuity of 'slow phagocytosis'. Also note the PtdIns(3)P-decorated thread-like structure between the phagosome and PtdIns(3)P-positive vesicles surrounding the phagosome. Images for the first 5 min are included in the video.

Mitosomes in *Entamoeba histolytica* contain a sulfate activation pathway

Fumika Mi-ichi, Mohammad Abu Yousuf, Kumiko Nakada-Tsukui, and Tomoyoshi Nozaki[1]

Department of Parasitology, National Institute of Infectious Diseases, Tokyo 162-8640, Japan

Edited by Andrew Roger, Dalhousie University, Halifax, NS, Canada, and accepted by the Editorial Board October 19, 2009 (received for review June 25, 2009)

Hydrogenosomes and mitosomes are mitochondrion-related organelles in anaerobic/microaerophilic eukaryotes with highly reduced and divergent functions. The full diversity of their content and function, however, has not been fully determined. To understand the central role of mitosomes in *Entamoeba histolytica*, a parasitic protozoon that causes amoebic dysentery and liver abscesses, we examined the proteomic profile of purified mitosomes. Using 2 discontinuous Percoll gradient centrifugation and MS analysis, we identified 95 putative mitosomal proteins. Immunofluorescence assay showed that 3 proteins involved in sulfate activation, ATP sulfurylase, APS kinase, and inorganic pyrophosphatase, as well as sodium/sulfate symporter, involved in sulfate uptake, were compartmentalized to mitosomes. We have also provided biochemical evidence that activated sulfate derivatives, adenosine-5′-phosphosulfate and 3′-phosphoadenosine-5′-phosphosulfate, were produced in mitosomes. Phylogenetic analysis showed that the aforementioned proteins and chaperones have distinct origins, suggesting the mosaic character of mitosomes in *E. histolytica* consisting of proteins derived from α-proteobacterial, δ-proteobacterial, and ancestral eukaryotic origins. These results suggest that sulfate activation is the major function of mitosomes in *E. histolytica* and that *E. histolytica* mitosomes represent a unique mitochondrion-related organelle with remarkable diversity.

anaerobic protozoa | evolution | mitochondria | organelle | proteomics

Diversification of mitochondrial structure and function has occurred during eukaryotic evolution, and was especially observed in anaerobic/microaerophilic environments. Most extant anaerobic eukaryotes, which were previously considered to lack mitochondria, are now regarded to possess reduced and highly divergent forms of mitochondrion-related organelles (1, 2). The hydrogenosome is an organelle in which hydrogen and ATP are produced, and is found in anaerobic protists and fungi such as *Trichomonas vaginalis* (3, 4), *Neocallimastix patriciarum* (5, 6), and *Nyctotherus ovalis* (7). The mitosome, typically demonstrated in parasitic and free-living protists such as *E. histolytica* (2, 8–15), *Giardia intestinalis* (16, 17), diverse microsporidian species (18–20), and *Cryptosporidium parvum* (21), generally has reduced functions and does not produce hydrogen or ATP. In *Mastigamoeba balamuthi*, a mitochondrion-related organelle was discovered and presumed to possess a unique array of biochemical properties, although it remains unclear whether the organelle is more similar to either hydrogenosomes or mitosomes (22). In contrast, the mitochondrion-related organelle in *Blastocystis* contains DNA and shows characteristics for both hydrogenosomes and mitochondria of higher eukaryotes (23). Organisms that possess hydrogenosomes and mitosomes do not cluster together in eukaryote phylogenies, indicating that secondary losses and changes in mitochondrial functions have independently occurred multiple times in eukaryote evolution (1). Although hydrogenosomes and mitosomes are divergent in their contents and functions, a number of shared characteristics have been previously suggested, which include a double membrane, mitochondrial chaperonin 60 (Cpn60), and the iron sulfur cluster (ISC) system (1). However, recent studies indicate that *E. histolytica* and *M. balamuthi* lack the ISC system, and instead possess the nitrogen fixation (NIF) system, which is most likely derived from an ancestral nitrogen fixing ε-proteobacterium by lateral gene transfer (22, 24). Only 5 proteins have been demonstrated in *E. histolytica* mitosomes: Cpn60 (8–10, 12), Cpn10 (13), mitochondrial Hsp70 (11, 15), pyridine nucleotide transhydrogenase (PNT) (2, 8), and mitochondria carrier family (MCF, ADP/ATP transporter) (14), and the central role of mitosomes in *E. histolytica* remains unknown. Analysis of the genome of *E. histolytica* has not revealed any additional information regarding the function of mitosomes and thus, a proteomic analysis of mitosomes seems to be the best approach to understand its structure and function (1, 2).

In this study, we examined the proteomic profile of purified mitosomes and showed by immunofluorescence assay that a repertoire of proteins were localized to mitosomes, and demonstrated by enzymological studies that some of these mitosomal proteins were associated with sulfate activation. We further showed by phylogenetic analysis that mitosomes are a mosaic organelle consisting of components derived from at least 3 distinct origins. This study identifies that sulfate activation is the major function of mitosomes in *E. histolytica*.

Results

Identification of Mitosomal Proteins. To elucidate the central role of mitosomes in *E. histolytica*, we took a proteomic approach to identify the proteins associated with mitosomes. We developed an improved purification scheme, consisting of 2 consecutive discontinuous Percoll gradient centrifugations that yielded an enriched mitosomal fraction suitable for proteome analysis [supporting information (SI) Fig. S1]. The presence of mitosomes was monitored with the authentic mitosomal marker Cpn60. Mitosomes were recovered from fractions 19 and 20 in the first centrifugation and from fractions I through K in the second centrifugation with a peak in fraction J (Fig. 1). A list of mitosomal proteins was made by subtracting the proteins identified in fractions G and O from those in fraction J, as fraction J contained traces of either lysosome or ER protein, which were detected by markers cysteine protease 5 (CP5) and Sec61α, respectively (Fig. 1).

Survey of the Mitosomal Proteome. Three independent mitosomal purifications and MS analysis reproducibly identified 95 putative mitosomal proteins (Table S1). Although 64 of the proteins identified were annotated in the *E. histolytica* genome database as "hypothetical protein," 3 enzymes involved in sulfate activation—ATP sulfurylase (AS) (25), APS kinase (APSK), and inorganic pyrophosphatase (IPP)—were identified as dominant constituents, based on the high coverage obtained for each protein (as described

Author contributions: F.M. and T.N. designed research; F.M., M.A.Y., and K.N.-T. performed research; F.M. contributed new reagents/analytic tools; F.M. and T.N. analyzed data; and F.M. and T.N. wrote the paper.

The authors declare no conflict of interest.

This article is a PNAS Direct Submission. A.R. is a guest editor invited by the Editorial Board.

[1]To whom correspondence should be addressed. E-mail: nozaki@nih.go.jp.

This article contains supporting information online at www.pnas.org/cgi/content/full/0907106106/DCSupplemental.

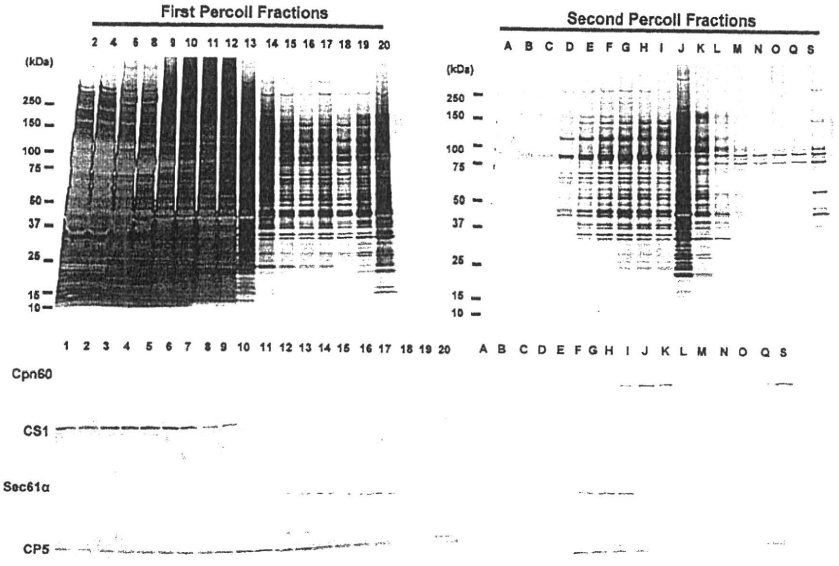

Fig. 1. Purification of mitosomes. Fractions derived from the first (fractions 1–20) and second (fractions A-S) discontinuous Percoll gradient centrifugation were electrophoresed on 5%–20% SDS/PAGE and subjected to immunoblot analyses using antibodies against well established organelle markers: Cpn60 (mitosome), cysteine synthase 1 (CS1; cytoplasm), Sec61α (endoplasmic reticulum), and CP5 (lysosome).

later). Three transporters and 7 metabolic enzymes were also identified. In addition, 7 proteins involved in membrane trafficking, including 4 Rab family GTPases, were detected. Furthermore, a weak homologue of Tom40 (expectation value of 0.13), a component of the transport complex of the outer membrane of the mitochondria, was identified. Three chaperones, Cpn60, Cpn10, mitochondrial Hsp70, and MCF, which were previously reported as *Entamoeba* mitosomal proteins (12–15), were also confirmed. Conversely, PNT and 2 proteins involved in the NIF system—NifS and NifU—were not detected. The proteome described here is likely to be partial, as only proteins enriched in fraction J were considered as mitosomal proteins, although Cpn60 was detected throughout fractions I through S in the second gradient (Fig. 1). The heterogeneity displayed by mitosomes in the immunofluorescence assay (described later) also indicates that other subfractions of mitosomes have likely been excluded from the list.

Verification of the Mitosomal Localization of the Identified Proteins. To confirm the cellular localization of these proteins, 21 randomly chosen putative mitosomal proteins and 4 known mitosomal proteins were examined by immunofluorescence assay in *E. histolytica* cell lines expressing HA-tagged proteins. Among the 25 proteins examined, 22 proteins—including MCF, mitochondrial Hsp70, and Cpn10—colocalized with the mitosomal marker Cpn60 (Fig. 2, Fig. S2, and Table S1). These results validated our proteomic approach for the identification of mitosomal proteins.

The distribution of each protein in mitosomes was not uniform. We often observed variations in the signal intensity between Cpn60 and other mitosomal proteins including mitochondrial Hsp70 and MCF (Fig. 2 *C* and *G* and Fig. S2 *C*, *G*, *K*, and *O*). These observations indicated that the composition of mitosomes is not homogeneous. The heterogeneity in the distribution of individual mitosomal proteins was not a result of the overexpression of the HA-tagged proteins, because endogenous and HA-tagged Cpn60 were well co-localized (Fig. 2 *I–L*).

Compartmentalization of the Sulfate Activation Pathway in Mitosomes. AS, APSK, and IPP were identified as dominant constituents of mitosomes by proteomic analysis. Immunofluorescence imaging of *E. histolytica* cell lines expressing HA-tagged AS, APSK, and IPP revealed small punctate signals throughout the cytoplasm, which co-localized well with Cpn60 (Fig. 2 *A–H* and Fig. S2 *A–D*). Furthermore, XP_655928, one of the 5 putative sodium/sulfate symporters identified in the *E. histolytica* genome (XP_649603, XP_654527, XP_654503, XP_655928, and XP_657578), colocalized with Cpn60, suggesting its involvement in the uptake and transport of sulfate into mitosomes (Fig. S2 *E–H*).

To further demonstrate the presence of a functional sulfate activation pathway compartmentalized to mitosomes, AS and APSK activities were measured in the Percoll gradient centrifugation fractions using $Na_2[^{35}S]O_4$. Both [^{35}S]-labeled adenosine-5′-phosphosulfate (APS) and 3′-phosphoadenosine-5′-phosphosulfate (PAPS) were detected (Fig. 3). PAPS was predominantly detected in fractions 19 and 20 of the first centrifugation and fractions I through K of the second centrifugation (Fig. 3). The distribution of the PAPS-forming activity was similar to Cpn60 (Fig. 1). In contrast, APS was detected in nearly all fractions (i.e., D-S) of the second centrifugation. This suggests that AS is not exclusively localized to mitosomes, despite its clear mitosomal localization observed by immunofluorescence analysis. Alternatively, APS synthesis may be partially catalyzed by an unidentified protein.

Identification of Metabolites of Activated Sulfate. To examine the fate of activated sulfate in *E. histolytica*, we incubated trophozoites in

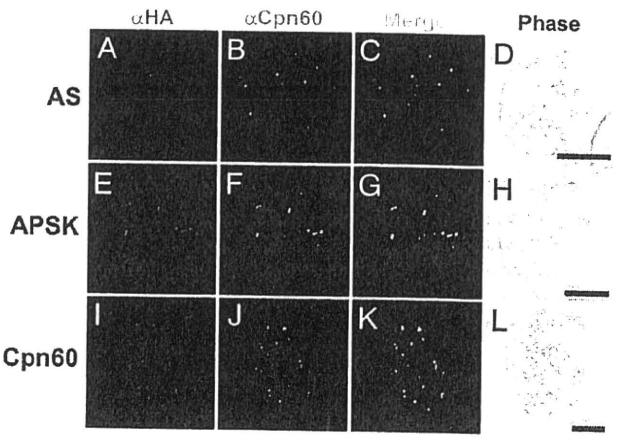

Fig. 2. Immunolocalization of representative mitosomal proteins. Colocalization of individual mitosomal proteins with the HA epitope (anti-HA antibody, red) and the authentic mitosomal protein marker Cpn60 (native Cpn60 antiserum, green) is shown (*A–H*). Colocalization of endogenous Cpn60 and exogenous HA-tagged Cpn60 is also shown (*I–L*). (Scale bars: 10 μm.)

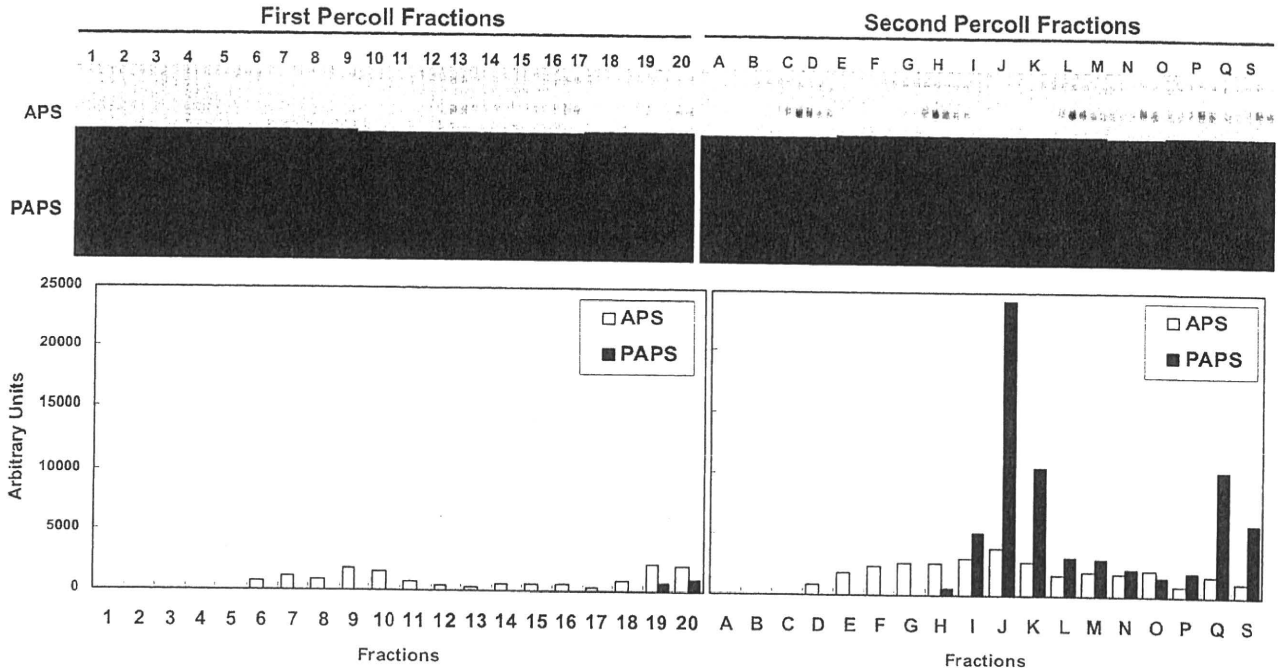

Fig. 3. Demonstration of AS and APSK activities. Mitosome-enriched fractions were tested for the ability to synthesize ^{35}S-labeled APS or PAPS (26). The reaction mixture for each sample totaled 12 μL and contained 39 mM $MgCl_2$, 64 mM ATP, 1.3 mM Na_2SO_4 (25 mCi/m mole), and 20 mM Tris/HCl (pH 8.0). The reaction was initiated by the addition of the freeze-thawed fraction (3 μL), carried out for 2 h at 25 °C, and terminated by the addition of 88 μL methanol. Ten-microliter samples were analyzed by PEI-cellulose TLC to determine ^{35}S-labeled APS or PAPS as previously described (27). The amount of each product was quantified by densitometric analysis using an image analyzer (Fuji) and the results are expressed in arbitrary units.

BI-S-33 medium containing $Na_2[^{35}S]O_4$ for up to 2 h, or labeled for 1 h and chased for up to 24 h. The cell lysate was separated into methanol-soluble and insoluble fractions. Labeled [^{35}S] was detected predominantly in the methanol-soluble fraction. At least 5 polar lipids, separated on a silica HPTLC plate in 25:65:10 (vol/vol/vol) methanol/chloroform/acetic acid (Fig. 4), accounted for most of the [^{35}S] detected (81.6% ± 6.2% at 1 h pulse). These lipids were distinct from commonly observed phospholipid species (phosphatidylethanolamine, phosphatidylserine, phosphatidylinositol, and phosphatidylcholine). These data indicate that activated sulfate is mainly used to synthesize sulfur-containing polar lipids.

Phylogenetic Analysis of the Sulfate Activation Pathway. To investigate the origin of sulfate activation in *E. histolytica*, phylogenetic analyses of the proteins involved in the pathway and established mitosomal chaperones were conducted. The origins of AS, APSK, IPP, sodium/sulfate symporter, Cpn60, and mitochondrial Hsp70 were not identical. *E. histolytica* AS showed strong affinity to AS from δ-proteobacteria (Fig. 5), whereas *E. histolytica* IPP clustered with IPP from other eukaryotes (Fig. S4). *E. histolytica* APSK was closely related to δ-proteobacteria, α-proteobacteria, and *Dictyostelium discoideum* (with low bootstrap values), and *E. histolytica* sodium/sulfate symporters clustered with a limited group of eukaryotes (diatoms and green algae) and bacteria, although their exact origins were not clearly resolved (Fig. S3 and Fig. S5). In contrast, *E. histolytica* Cpn60 and mitochondrial Hsp70 showed monophyly with the α-proteobacteria (8, 11, 22). The data indicate the phylogenetically mosaic nature of mitosomes in *E. histolytica*.

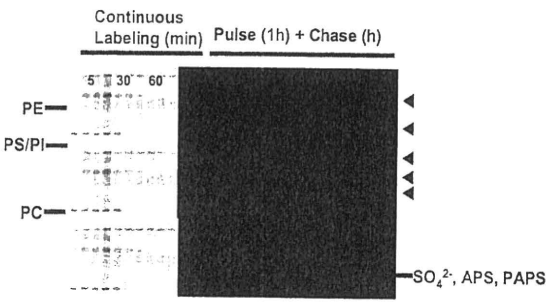

Fig. 4. Incorporation of [^{35}S]-labeled sulfate into polar lipids. ^{35}S was incorporated into at least 5 polar lipids (arrowheads), which were distinct from commonly observed phospholipid species. PE, phosphatidylethanolamine; PS, phosphatidylserine; PI, phosphatidylinositol; PC, phosphatidylcholine.

Discussion

Although the diversity in structure and function of mitochondrion-related organelles have been demonstrated in a wide range of organisms, *E. histolytica* remains as one of the anaerobic/microaerophilic eukaryotes, in which the function of the mitochondrion-related organelle remains unknown. In this study, we have provided biochemical and microscopic evidence demonstrating that sulfate activation, which generally occurs in the cytoplasm and plastids in eukaryotes, is the major function of mitosomes in *E. histolytica*.

Genes encoding for all of the major components necessary for sulfate activation and transport of substrates and products across the mitosomal membrane are identifiable in the genome (Fig. 6). Sodium/sulfate symporter, which is necessary for the uptake of sulfate into mitosomes, was identified. ATP that is necessary for the activation of sulfate by both AS and APSK, and the quality control of heat-sensitive AS by chaperones, is incorporated via MCF to mitosomes with a concomitant cytosolic export of ADP or AMP. *E. histolytica* MCF transports both ADP and AMP to the cytosol for the incorporation of ATP to mitosomes (14). In other organisms, PAPS transporter (PAPST), which transports PAPS and AMP in opposite directions, is required for shuttling PAPS between the

EVOLUTION

Fig. 5. Phylogenetic analysis of AS. The best maximum likelihood (*ML*) tree of AS inferred by the JTT model taking across-site rate heterogeneity into consideration. The α-value of the Γ-shaped parameter used in the analysis of AS was 0.50723. Bootstrap proportion (*BP*) values are attached to the internal branches. Branches with less than 50% BP support are unmarked. BP values are calculated by ML, distance matrix (*DM*), and maximum parsimony (*MP*) methods. One hundred and 1,000 resamplings were performed for ML and DM and MP analyses, respectively. The length of each branch is proportional to the estimated number of substitution. With 67 taxa, 302 aligned amino acid sites were used for analysis, corresponding to residues 55 to 103, 117 to 131, 135 to 147, 151 to 178, 182 to 196, 200 to 226, 231 to 262, 264 to 325m and 333 to 399 of the *E. histolytica* sequence.

organelle and the cytosol (28). Although the *E. histolytica* genome contains a gene encoding for putative PAPST (XP_654175; expectation value, 4.2^{-14}) (29, 30), we failed to demonstrate the mitosomal localization of the protein (PAPST; Fig. S6). In addition, a putative phosphate transporter (XP_654379; expectation value, 1.23^{-61}) (31) also failed to localize to mitosomes (PHT; Fig. S6). Thus, the identity of the presumptive PAPS and phosphate transporters in *E. histolytica* mitosomes remains unknown. Generally, PAPS is used in 2 different pathways. In one route, the sulfate moiety of PAPS is transferred to various acceptors to yield mucopolysaccharides, sulfolipids, and sulfoproteins by sulfotransferases. Alternatively, sulfate is reduced and assimilated into cysteine (32, 33). The *E. histolytica* genome contains 11 potential genes encoding for sulfotransferases, but lacks the enzymes for sulfate reduction (34, 35). Therefore, together with the results of $[^{35}S]O_4$ metabolic labeling (Fig. 4), it is conceivable to assume that PAPS predominantly serves as the sulfo-donor of sulfotransferases to synthesize sulfur-containing lipids. Two of the most highly expressed sulfotransferases (SULT1, XP_654200, expectation value, 1^{-12}; SULT2, XP_654101, expectation value, 1^{-13}) were distributed to the cytoplasm (SULT1 and SULT2; Fig. S6), suggesting that sulfo-transfer reactions occur in the cytosol, and thus reinforcing the premise that PAPS needs to be exported from mitosomes. Further characterization of these sulfur-containing lipid species in *E. histolytica* is necessary to understand the physiological significance of the compartmentalized sulfate activation in mitosomes of this organism.

As sulfate activation in eukaryotes generally occurs in the cytoplasm and plastids (36, 37), our finding has raised an important question on whether compartmentalization of sulfate activation in mitosomes is unique to *E. histolytica*. The acquisition and compart-

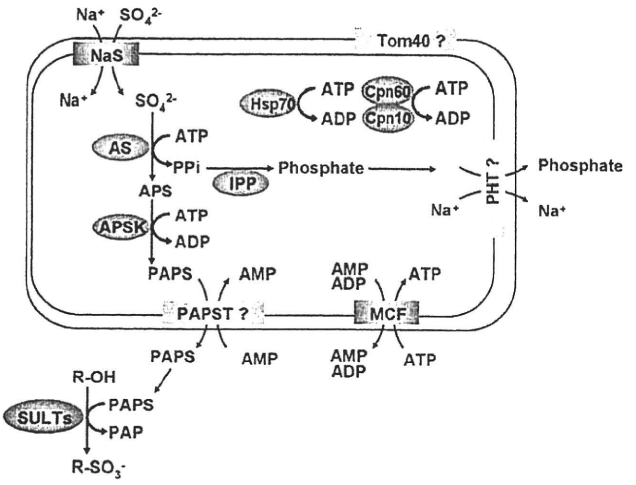

Fig. 6. A compartmentalized sulfate activation pathway in *E. histolytica* mitosomes. The mitosome proteins whose localization was confirmed by immunofluorescence assay are shown in red, whereas the putative transporters are shown in gray. PHT, phosphate transporter; SULT, sulfotransferase. Two of the most highly expressed sulfotransferases were demonstrated to be localized to the cytoplasm (Fig. S6).

mentalization of the enzymes involved in sulfate activation may have occurred exclusively in *Entamoeba* among the anaerobic/microaerophilic organisms possessing mitochondrion-related organelles. *T. vaginalis*, *G. intestinalis*, and *C. parvum* apparently lack genes encoding for the enzymes. *Encephalitozoon cuniculi*, one of the microsporidia, has the gene for IPP (Fig. S4), but lacks genes encoding for AS and APSK. Although the genome and EST databases are not complete for *M. balamuthi* and *N. patriciarum*, none of *AS*, *APSK*, and *IPP* genes was found so far. It is worth examining if genes involved in sulfate activation are present in *M. balamuthi* because the 2 species share the NIF system for FeS cluster biosynthesis (22). There is only one eukaryote, other than *E. histolytica*, that possesses sulfate activation in the mitochondria. In *Euglena gracilis*, the enzymatic activities involved in sulfate activation and reduction have been detected in the mitochondria (36, 38, 39). The origin of *E. gracilis* AS, however, is presumed to be the secondary green algal plastid and not the δ-proteobacteria (36), whereas *E. gracilis* IPP is thought to be derived from bacteria and not an ancestral eukaryote (Fig. S4). These results suggest that the origins of *E. gracilis* mitochondria are distinct from those of *E. histolytica* mitosomes. Based on the fact that the 4 *E. histolytica* proteins involved in sulfate transport and activation have origins distinct from α-proteobacterium, we propose a hypothesis whereby AS, APSK, and sodium/sulfate symporter were acquired by the ancestor of *Entamoeba* from δ-proteobacterium (and other bacteria) by lateral gene transfer (40). We examined whether AS and APSK were found in an operon in δ-proteobacteria, which would support the hypothesis whereby both AS and APSK of δ-proteobacterial origin were transferred to the ancestor of *Entamoeba*. However, this is not a case in at least 2 representative species (*Desulfotalea psychrophila* and *Desulfovibrio vulgaris*).

Various diverse or sometimes shared characteristics are reported in other eukaryotes possessing either hydrogenosomes or mitosomes. These include hydrogenase and pyruvate:ferredoxin oxidoreductase for ATP generation in hydrogenosomes; NADH dehydrogenase part of mitochondrial complex I in *T. vaginalis*, *N. ovalis*, and *Blastocystis*; TCA cycle enzymes in *M. balamuthi*, *Blastocystis*, *N. patriciarum*, *and N. ovalis*; glycine cleavage complex in *M. balamuthi*, *T. vaginalis*, and *Blastocystis*; and alternative oxidase in *Blastocystis* and *C. parvum* (1). Cpn60 and the ISC system were thought to be shared characteristics of hydrogenosomes and mitosomes in anaerobic/microaerophilic eukaryotes (1). However, *E. histolytica* and *M. balamuthi* possess only the NIF system instead of the ISC system (22, 24). In the mitosomal proteome, neither NifS nor NifU was identified in the mitosome-enriched fraction. We previously reported that NifS and NifU, both of which lack a mitochondrion-targeting signal, were fractionated on an anion exchange chromatography from the soluble fraction obtained by 0.45-μm filtration and 45,000 × *g* ultracentrifugation of amoebic lysate, suggesting the predominantly cytoplasmic localization of the NIF system in *E. histolytica* (24). Similarly, both NifS and NifU in *M. balamuthi* lack a mitochondria targeting signal (22). These data suggest that FeS cluster biosynthesis in *E. histolytica* and *M. balamuthi* are mainly, if not exclusively, localized to the cytosol (22, 24). However, it remains unknown whether the *E. histolytica* mitosomes also partially contain the NIF system.

The targeting mechanisms to the *E. histolytica* mitosomes remain unsolved and need further investigation. Although *Entamoeba* PNT was presumed to be imported into mitosomes based on the resemblance of its amino-terminal portion rich in hydroxylated and basic amino acids to the canonical mitochondrial targeting peptide (2), our proteomic and immunofluorescence studies clearly showed that PNT is not imported to mitosomes, but is distributed to vesicles and vacuoles (Fig. S7). Commonly available prediction programs such as Mitoprot (41) and PSORT II (42) were unable to correctly predict the mitosomal localization of proteins whose localization was verified by immunofluorescence assay. Similarly, the remaining putative mitosomal proteins have no predictable mitochondrial targeting signal. As described earlier, our mitosomal proteome contained a weak homologue of Tom40 (expectation value, 0.13). Thus, there is a need to verify the identity of this potential Tom40 and the existence of the Tom complex in *E. histolytica*. In other anaerobic eukaryotes, protein import machinery to the mitochondrion-related organelles appears to be conserved (43, 44), and the mitosomal targeting signal from *G. lamblia* and the hydrogenosome targeting signal from *T. vaginalis* were interchangeable (45). On the contrary, cryptic mitochondrial targeting signals have also been discovered in *G. lamblia*, T. vaginalis, and microsporidian species, and unique aspects of mitochondrial processing peptidases have been reported in *G. lamblia* (1, 46). Together, the machinery and mechanisms of protein import into mitosomes require further investigation.

In summary, we have shown that *E. histolytica* mitosomes are a mitochondrion-related organelle that is highly divergent and represents a mosaic organelle consisting of proteins derived from α-proteobacteria, δ-proteobacteria, and eukaryotes. It is primarily involved in sulfate activation. This study should shed light on the diversification of mitochondrion-related organelles in eukaryotic evolution.

Materials and Methods

Mitosome Purification. Approximately 0.5–1 × 10^8 trophozoites of *E. histolytica* strain HM-1:IMSS cl6 (47), cultivated axenically in Diamond BI-S-33 medium (48), were resuspended in 1 mL of homogenate buffer [250 mM sucrose, protease inhibitor mixture (Roche), 300 μM E-64, 10 mM Mops-KOH (pH 7.4)], and homogenized with a Dounce homogenizer. Unbroken cells, nuclei, and large vacuoles were removed by centrifugation at 5,000 × *g* at 4 °C for 10 min, and the supernatant was gently layered onto 3 mL of homogenization buffer containing 30% (vol/vol) Percoll. After centrifugation at 120,000 × *g* at 4 °C for 1 h, 200 μL fractions were collected from top to bottom (fractions 1–20). Fractions 19 and 20 (density >1.054) were collected, mixed, and applied onto 2 mL of homogenization buffer containing 70% (vol/vol) Percoll. The gradient was subsequently overlaid with 1 mL of the homogenization buffer containing 15% (vol/vol) Percoll. After centrifugation at 120,000 × *g* at 4 °C for 1 h, 200 μL of fractions were collected from top to bottom (fractions A-S; Fig. S1).

Immunoblot Analysis. Fractions prepared as previously mentioned were mixed with 4× SDS/PAGE sample buffer. Samples were boiled at 95 °C for 5 min followed by centrifugation at 13,000 × *g* at 4 °C for 20 min to remove the Percoll. The fractions were analyzed by SDS/PAGE, silver stained, and immunoblot analysis as

EVOLUTION

previously described (49). The dilution of the primary antibodies was 1:1,000 for anti-Cpn60 and anti-cysteine synthase 1 antiserum, and 1:100 for anti-CP5 and anti-Sec61α antiserum (50, 51).

Production of *E. histolytica* Lines Expressing Epitope-Tagged Mitosomal Proteins. Plasmids for the production of amoeba lines expressing engineered mitosomal proteins containing 3 tandem HA-epitopes were constructed essentially as previously described (52). Lipofection of trophozoites and selection of transformants were also performed as previously described (53).

Indirect Immunofluorescence Assay. Indirect immunofluorescence assay was performed as previously described (49) with some modifications. Briefly, the amoebae were washed and fixed with acetone/methanol (1:1) for 10 min. After washing with PBS solution, cells were permeabilized with 0.3% Triton X-100 for 15 min and reacted with primary antibody diluted at 1:500 (anti-Cpn60 antiserum) and 1:1,000 (anti-HA monoclonal antibody) in PBS solution. The samples were then reacted with Alexa Fluor 488- or 568-conjugated anti-rabbit or anti-mouse secondary antibody (1:1,000) for 1 h. The samples were examined as previously described (49).

Metabolic Labeling. Approximately 10^6 trophozoites were labeled with [^{35}S]-labeled sulfate (25 mCi/m mole) in 0.5 mL of the Diamond BI-S-33 medium either continuously for 5 to 120 min or labeled for 1 h and chased for 1 to 24 h (54). Cells were collected and lipids were extracted with 0.5 mL of methanol and separated on a silica high-performance thin-layer chromatography plate in 25:65:10 (vol/vol/vol) methanol/chloroform/acetic acid. Dried thin-layer chromatography plates were analyzed by autoradiography.

ACKNOWLEDGMENTS. We thank Dr. Takeshi Makiuchi for discussions of phylogenetic analysis. We thank Yoko Yamada, Kyoko Masuda, Kayoko Hashimoto, and Rumiko Kosugi for technical assistance. We thank Jorge Tovar, Royal Holloway University of London, for anti-Cpn60 antibody for an initial analysis of Cpn60. We also thank Rosana Sánchez-López, UNAM, Cuernavaca, Mexico, for anti-Sec61α antiserum. This work was supported by Creative Scientific Research Grant 18GS0314 from the Japanese Ministry of Education, Science, Culture, Sports, and Technology (to T.N.); Grant-in-Aid for Scientific Research (18GS0314, 18050006, 18073001) from the Ministry of Education, Culture, Sports, Science and Technology of Japan; a grant for research on emerging and re-emerging infectious diseases from the Ministry of Health, Labour and Welfare of Japan; and a grant for research to promote the development of anti-AIDS pharmaceuticals from the Japan Health Sciences Foundation (to T.N.).

1. van der Giezen M (2009) Hydrogenosomes and mitosomes: conservation and evolution of functions. *J Eukaryot Microbiol* 56:221–231.
2. Aguilera P, Barry T, Tovar J (2008) *Entamoeba histolytica* mitosomes: organelles in search of a function. *Exp Parasitol* 118:10–16.
3. Lindmark DG, Muller M (1973) Hydrogenosome, a cytoplasmic organelle of the anaerobic flagellate *Tritrichomonas foetus*, and its role in pyruvate metabolism. *J Biol Chem* 248:7724–7728.
4. Hrdy I, et al. (2004) *Trichomonas* hydrogenosomes contain the NADH dehydrogenase module of mitochondrial complex I. *Nature* 432:618–622.
5. Yarlett N, Orpin CG, Munn EA, Yarlett NC, Greenwood CA (1986) Hydrogenosomes in the rumen fungus *Neocallimastix patriciarum*. *Biochem J* 236:729–739.
6. van der Giezen M, et al. (2003) Fungal hydrogenosomes contain mitochondrial heat-shock proteins. *Mol Biol Evol* 20:1051–1061.
7. Hackstein JH, Tjaden J, Huynen M Mitochondria, hydrogenosomes and mitosomes: products of evolutionary tinkering! *Curr Genet* 50:225–245, 2006.
8. Clark CG, Roger AJ (1995) Direct evidence for secondary loss of mitochondria in *Entamoeba histolytica*. *Proc Natl Acad Sci USA* 92:6518–6521.
9. Mai, Z, et al. (1999) Hsp60 is targeted to a cryptic mitochondrion-derived organelle ("crypton") in the microaerophilic protozoan parasite *Entamoeba histolytica*. *Mol Cell Biol* 19:2198–2205.
10. Tovar J, Fischer A, Clark CG (1999) The mitosome, a novel organelle related to mitochondria in the amitochondrial parasite *Entamoeba histolytica*. *Mol Microbiol* 32:1013–1021.
11. Bakatselou C, Kidgell C, Clark CC (2000) A mitochondrial-type hsp70 gene of *Entamoeba histolytica*. *Mol Biochem Parasitol* 110:177–182.
12. Leon-Avila G, Tovar J (2004) Mitosomes of *Entamoeba histolytica* are abundant mitochondrion-related remnant organelles that lack a detectable organellar genome. *Microbiology* 150:1245–1250.
13. van der Giezen M, Leon-Avila G, Tovar J (2005) Characterization of chaperonin 10 (Cpn10) from the intestinal human pathogen *Entamoeba histolytica*. *Microbiology* 151:3107–3115.
14. Chan KW, et al. (2005) A novel ADP/ATP transporter in the mitosome of the microaerophilic human parasite *Entamoeba histolytica*. *Curr Biol* 15:737–742.
15. Tovar J, Cox SS, van der Giezen M (2007) A mitosome purification protocol based on percoll density gradients and its use in validating the mitosomal nature of *Entamoeba histolytica* mitochondrial Hsp70. *Methods Mol Biol* 390:167–177.
16. Tovar J, et al. (2003) Mitochondrial remnant organelles of *Giardia* function in iron-sulphur protein maturation. *Nature* 426:172–176.
17. Dolezal P, et al. (2005) *Giardia* mitosomes and trichomonad hydrogenosomes share a common mode of protein targeting. *Proc Natl Acad Sci USA* 102:10924–10929.
18. Burri L, Williams BA, Bursac D, Lithgow T, Keeling PJ (2006) Microsporidian mitosomes retain elements of the general mitochondrial targeting system. *Proc Natl Acad Sci USA* 103:15916–15920.
19. Goldberg AV, et al. (2008) Localization and functionality of microsporidian iron-sulphur cluster assembly proteins. *Nature* 452:624–628.
20. Tsaousis AD, et al. (2008) A novel route for ATP acquisition by the remnant mitochondria of. *Encephalitozoon cuniculi*. *Nature* 453:553–556.
21. Henriquez FL, Richards TA, Roberts F, McLeod R, Roberts CW (2005) The unusual mitochondrial compartment of *Cryptosporidium parvum*. *Trends Parasitol* 21:68–74.
22. Gill EE, et al. (2007) Novel mitochondrion-related organelles in the anaerobic amoeba *Mastigamoeba balamuthi*. *Mol Microbiol* 66:1306–1320.
23. Stechmann A, et al. (2008) Organelles in *Blastocystis* that blur the distinction between mitochondria and hydrogenosomes. *Curr Biol* 18:580–585.
24. Ali V, Shigeta Y, Tokumoto U, Takahashi Y, Nozaki T (2004) An intestinal parasitic protist, *Entamoeba histolytica*, possesses a non-redundant nitrogen fixation-like system for iron-sulfur cluster assembly under anaerobic conditions *J Biol Chem* 279:16863–16874.
25. Nozaki T, et al. (1998) Cloning and bacterial expression of adenosine-5′-triphosphate sulfurylase from the enteric protozoan parasite *Entamoeba histolytica*. *Biochim Biophys Acta* 1429:284–291.
26. Leyh TS, Taylor JC, Markham GD (1988) The sulfate activation locus of *Escherichia coli* K12: cloning, genetic, and enzymatic characterization. *J Biol Chem* 263:2409–2416.
27. Yanagisawa K, et al. (1998) cDNA cloning, expression, and characterization of the human bifunctional ATP sulfurylase/adenosine 5′-phosphosulfate kinase enzyme. *Biosci Biotechnol Biochem* 62:1037–1040.
28. Capasso JM, Hirschberg CB (1984) Mechanisms of glycosylation and sulfation in the Golgi apparatus: evidence for nucleotide sugar/nucleoside monophosphate and nucleotide sulfate/nucleoside monophosphate antiports in the Golgi apparatus membrane. *Proc Natl Acad Sci USA* 81:7051–7055.
29. Kamiyama S, et al. (2003) Molecular cloning and identification of 3′-phosphoadenosine 5′-phosphosulfate transporter. *J Biol Chem* 278:25958–25963.
30. Kamiyama S, et al. (2006) Molecular cloning and characterization of a novel 3′-phosphoadenosine 5′-phosphosulfate transporter, PAPST2. *J Biol Chem* 281:10945–10953.
31. Guo B, Irigoyen S, Fowler TB, Versaw WK (2008) Differential expression and phylogenetic analysis suggest specialization of plastid-localized members of the PHT4 phosphate transporter family for photosynthetic and heterotrophic tissues. *Plant Signal Behav* 3:784–790.
32. Strott CA (2002) Sulfonation and molecular action. *Endocr Rev* 23:703–732.
33. Negishi M, et al. (2001) Structure and function of sulfotransferases. *Arch Biochem Biophys* 390:149–157.
34. Clark CG, et al. (2007) Structure and content of the *Entamoeba histolytica* genome. *Adv Parasitol* 65:51–190.
35. Ali V, Nozaki T (2007) Current therapeutics, their problems, and sulfur-containing-amino-acid metabolism as a novel target against infections by "amitochondriate" protozoan parasites. *Clin Microbiol Rev* 20:164–187.
36. Patron NJ, Durnford DG, Kopriva S (2008) Sulfate assimilation in eukaryotes: fusions, relocations and lateral transfers. *BMC Evol Biol* 8:1–14.
37. Bradley ME, Rest JS, Li WH, Schwartz NB (2009) Sulfate activation enzymes: phylogeny and association with pyrophosphatase. *J Mol Evol* 68:1–13.
38. Brunold C, Schiff JA (1976) Studies of sulfate utilization of algae: 15. Enzymes of assimilatory sulfate reduction in *Euglena* and their cellular localization. *Plant Physiol* 57:430–436.
39. Saidha T, Na SQ, Li JY, Schiff JA (1988) A sulphate metabolizing centre in *Euglena* mitochondria. *Biochem J* 253:533–539.
40. Loftus B, et al. (2005) The genome of the protist parasite. *Entamoeba histolytica Nature* 433:865–868.
41. Claros MG, Vincens P (1996) Computational method to predict mitochondrially imported proteins and their targeting sequences. *Eur J Biochem* 241:779–786.
42. Nakai K, Horton P (1999) PSORT: a program for detecting sorting signals in proteins and predicting their subcellular localization. *Trends Biochem Sci* 24:34–36.
43. Dolezal, et al. (2006) Evolution of the molecular machines for protein import into mitochondria. *Science* 313:314–318.
44. Dagley MJ, et al. (2009) The protein import channel in the outer mitosomal membrane of *Giardia intestinalis*. *Mol Biol Evol* 26:1941–1947.
45. Dolezal P, et al. (2005) *Giardia* mitosomes and trichomonad hydrogenosomes share a common mode of protein targeting. *Proc Natl Acad Sci USA* 102:10924–10929.
46. Smid O, et al. (2008) Reductive evolution of the mitochondrial processing peptidases of the unicellular parasites *Trichomonas vaginalis* and *Giardia intestinalis*. *PLoS Pathog* 4: e1000243.
47. Diamond LS, Mattern CF, Bartgis IL (1972) Viruses of *Entamoeba histolytica*. I. Identification of transmissible virus-like agents. *J Virol* 9:326–341.
48. Diamond LS, Harlow DR, Cunnick CC (1978) A new medium for the axenic cultivation of *Entamoeba histolytica* and other. *Entamoeba Trans R Soc Trop Med Hyg* 72:431–432.
49. Nakada-Tsukui K, Saito-Nakano Y, Ali V, Nozaki T (2005) A retromerlike complex is a novel Rab7 effector that is involved in the transport of the virulence factor cysteine protease in the enteric protozoan parasite *Entamoeba histolytica*. *Mol Biol Cell* 16:5294–5303.
50. Nozaki T, et al. (1998) Molecular cloning and characterization of the genes encoding two isoforms of cysteine synthase in the enteric protozoan parasite *Entamoeba histolytica*. *Mol Biochem Parasitol* 97:33–44.
51. Mitra BN, Saito-Nakano Y, Nakada-Tsukui K, Sato D, Nozaki T (2007) Rab11B small GTPase regulates secretion of cysteine proteases in the enteric protozoan parasite *Entamoeba histolytica*. *Cell Microbiol* 9:2112–2125.
52. Saito-Nakano Y, Yasuda T, Nakada-Tsukui K, Leippe M, Nozaki T (2004) Rab5-associated vacuoles play a unique role in phagocytosis of the enteric protozoan parasite *Entamoeba histolytica*. *J Biol Chem* 279:49497–49507.
53. Nozaki T, et al. (1999) Characterization of the gene encoding serine acetyltransferase, a regulated enzyme of cysteine biosynthesis from the protist parasites *Entamoeba histolytica* and *Entamoeba dispar*. Regulation and possible function of the cysteine biosynthetic pathway in *Entamoeba*. *J Biol Chem* 274:32445–32452.
54. Bakker-Grunwald T, Geilhorn B (1992) Sulfate metabolism in *Entamoeba histolytica*. *Mol Biochem Parasitol* 53:71–78.

原虫感染とIL-12サイトカインファミリー

The role of IL-12 cytokine family in protozoa infection

吉田裕樹・濱野真二郎

Th1型CD4陽性細胞は，インターフェロン-γを産生することにより細胞内寄生性原虫の排除に重要な細胞性免疫をつかさどっている．IL-12サイトカインファミリーメンバーは，Th1分化誘導作用をもつとともに，炎症誘導や免疫抑制など多彩な作用をもつ．IL-12はTh1の分化と維持に重要なサイトカインであり，原虫に対する感染防御に不可欠なサイトカインである．IL-27は，原虫感染時の過剰な免疫応答を制御し，致死的な炎症から宿主を守る機能ももっている．IL-12ファミリーサイトカインは，T細胞の分化や免疫反応を制御することにより，原虫感染においてさまざまな役割を果たしている．

Key words ●原虫 ●サイトカイン ●IL-12 ●Th1 ●免疫抑制

はじめに

原虫（原生動物）は単核の真核生物で，原生生物界に区分される．原虫のなかにはヒトを含む動物に寄生するものがあり，病原性をもつ原虫はときに感染症をひき起こす．ヒトにおいては，赤痢アメーバによるアメーバ赤痢，トリパノソーマ類によるアフリカ睡眠病やシャーガス病，リーシュマニア類による内臓/皮膚/皮膚粘膜型リーシュマニア症，各種マラリア原虫によるマラリアなどが，重篤な原虫感染症として知られている．

原虫に対する防御免疫のなかでは，CD4陽性ヘルパーT細胞（Th）が重要な役割を果たすことが知られている．ナイーブCD4陽性細胞が抗原を認識し活性化すると，Th1およびTh2という，2つの異なる性格をもつ細胞群に分化することが知られていた．原虫感染に関しては，Th1が産生するインターフェロン（IFN）-γによりマクロファージなどの食細胞が活性化し，細胞内寄生性原虫*1を排除する機構が重要である．近年，Th1/2と性質を異にするヘルパーT細胞集団Th17が同定された[1,2]．Th17は，炎症誘導にかかわるインターロイキン（IL）-17を産生し，好中球の遊走を介して細胞外病原体の排除に関与する．

こうしたT細胞の分化には，IL-12ファミリーサイトカインやIL-4などのサイトカインが重要な役割を果たしている．本稿では，IL-12ファミリーサイトカインの役割を概説し，とくに注目を集めているIL-27とIL-23を中心に，原虫感染におけるこれらのサイトカインのもつ多彩な機能について解説する．

Hiroki Yoshida[1], Shinjiro Hamano[2]
[1]佐賀大学医学部　分子生命科学講座，[2]九州大学大学院医学研究院感染免疫・熱帯医学分野
E-mail：yoshidah@med.saga-u.ac.jp
URL：www.mcis.med.saga-u.ac.jp

I IL-12サイトカインファミリー

1．リガンドと受容体

IL-12はp35とp40の2つのサブユニットからなり抗原提示細胞（antigen-presenting cell：APC）により産生される，1細胞群の誘導・維持に重要なサイトカインである．近年，IL-12類似サイトカインIL-23[3]，IL-27[4]，およびIL-35[5,6]が同定された．IL-23はp35様サブユニットp19とp40サブユニット（IL-12のp40と同一分子）からなる．IL-27は，p40様サブユニットEpstein-Barr virus-induced gene 3（EBI-3）とp35様サブユニットp28からなる．さらに近年になって，IL-12のp35とEBI-3からなるIL-35が同定された．IL-12，23，27は，活性化した樹状細胞などから産生されるが，IL-35は制御性T細胞（regulatory T cell：Treg）から産生されるとされている．

IL-12受容体は，β1とβ2の2つのサブユニットからなり，その下流では転写因子signal transducer and activator of transcription（STAT）4が活性化し，直接IFN-γ産生を誘導する．IL-23受容体は，IL-12受容体β1鎖，およびIL-23特異的受容体サブユニットからなり，その下流では，STAT1，3，4，5が活性化する．IL-27受容体は，WSX-1分子とIL-6受容体のシグナル伝達コンポーネントであるgp130からなり，その下流では，STAT1,3が活性化する．IL-35の受容体は同定されていない．

2. それぞれのサイトカインの機能

IL-12は，ナチュラルキラー（natural killer：NK）細胞やT細胞によるIFN-γ産生を誘導する，Th1分化に必須なサイトカインである[7]．

IL-23は，メモリータイプのT細胞によるIFN-γ産生を誘導すると報告されたが[3]，その後，Th17の分化を誘導することが明らかになった．Th17分化はIL-6＋TGF-β2より開始され，IL-23がその維持に必要であることがわかっている．

IL-27[4]は，STAT1を活性化することによりTh1特異的転写因子T-betの活性化を誘導し，Th1の分化を促進する[8]．IL-27には，このTh1分化誘導に加えて，Th17の分化抑制作用が認められる．WSX-1分子を欠損するマウスでは，Th17によってひき起こされる実験的自己免疫性脳脊髄炎*2が増悪し，また脳内でTh17が増加する[9,10]．さらに，IL-27は，IL-10産生誘導を介して，活性化T細胞によるサイトカイン産生を抑制する作用を有している[11~13]．

IL-35は，Th1誘導作用をもつとともに，Tregの増殖を誘導し，その一方でエフェクター細胞の増殖を抑制する[6]．またIL-35自体がTregから産生されるとされている[5]．IL-35は，IL-27と一部共通した作用を有しているが，その詳細に関しては不明な点が多い．図1に，IL-12，23，27，35，およびその受容体の構造とおもな役割を示す．

3. Th1分化と原虫感染免疫

Mosmannらにより，ナイーブCD4陽性細胞が，Th1とTh2という異なる性質をもつ2つの細胞集団に分かれることが報告されたのち[14]，その分化機構や生理的役割の詳細が明らかにされてきた．IL-12は，NK細胞やT細胞によるIFN-γ産生を誘導するサイトカインとして同定され，さらにTh1群の分化・維持に重要な役割を果たすことが明らかになった．IL-12刺激によりTh1などから産生されるIFN-γは，マクロファージなどに作用して，MHC分子の発現を上昇させるなどの機構によりその抗原提示能を亢進させるほか，誘導性一酸化窒素合成酵素（inducible nitric oxide synthase：iNOS）の発現を亢進させ，産生される一酸化窒素の作用などにより，さまざまな細胞内寄生性病原体の排除にかかわっている．Locksleyらのグループにより，*Leishmania major*に対して抵抗性を示すC57BL/6などのマウスにおいては感染時にTh1が分化

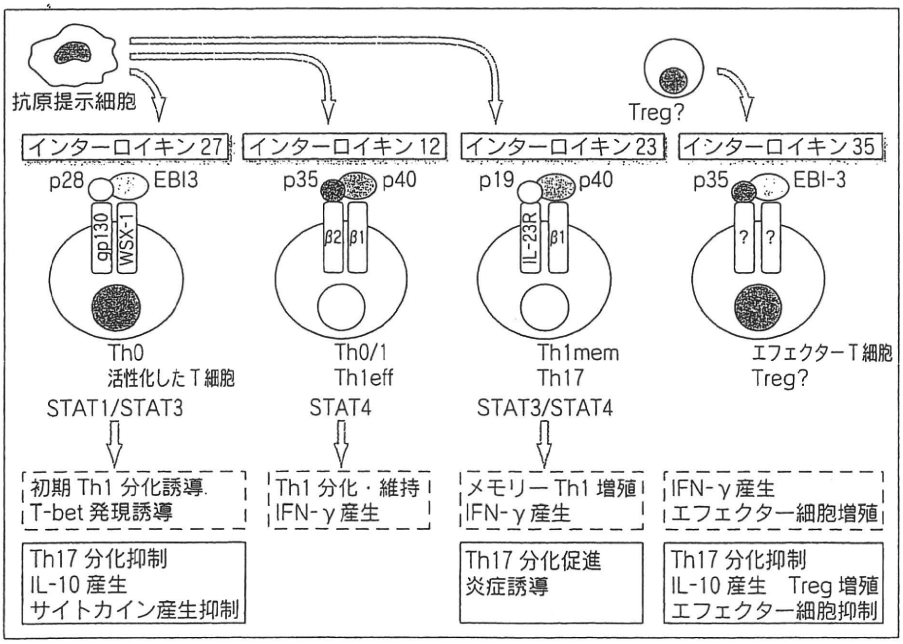

図1　IL-12/IL-12サイトカイン/受容体ファミリー

IL-12サイトカインファミリーメンバーとその受容体，活性化する転写因子を示す．IL-12，23，27は活性化した樹状細胞から産生される．IL-35は制御性T細胞（Treg）から産生されるとの報告がある．破線四角は，Th1分化に関する各サイトカインの役割，実線四角はTh1分化以外の役割を示す．IL-27は，活性化したT細胞に対してはサイトカイン産生抑制作用を示す．IL-23は，Th17に作用し，その分化を促進する．IL-35は，エフェクターT細胞に対する抑制作用と，Tregに対する増殖作用をもつ．Th1eff：エフェクターTh1，Th1mem：メモリーTh1．

*1　細胞内寄生性原虫：病原性細菌の一部には食細胞などに食菌されたのち，その殺菌機構をかいくぐって食細胞内で増殖できるものがある．本稿で示す原虫類のほか，結核菌，チフス菌などが知られ，感染時にはおもに細胞内で増殖し，病原性の発揮につながる．

*2　実験的自己免疫性脳脊髄炎：ミエリンオリゴ糖蛋白質などの神経関連蛋白質をマウスに免疫することにより発症する自己免疫性の脳脊髄炎．中枢神経系に炎症が生じ，四肢麻痺などを呈する．ヒトの多発性硬化症のモデルとして研究されている．

誘導されるが，感染感受性の高いBALB/cなどのマウスにおいてはTh1が誘導されないことが報告され，原虫感染防御におけるTh1の重要性が明確に示された[15]．*L. major*以外にも，*Trypanosoma cruzi*や*Toxoplasma gondii*など多くの細胞内寄生性原虫が，活性化したマクロファージ内で排除されることが知られている．

II 原虫感染におけるIL-12サイトカインファミリーの役割

これまでに，さまざまなサイトカインの生体内における役割が，サイトカインや抗サイトカイン抗体の投与，およびサイトカイン遺伝子欠損（ノックアウト：KO）マウスの解析などにより明らかにされてきた．KOマウスは遺伝子産物の機能を明らかにするうえで強力なツールであるが，IL-12サイトカインファミリーのようなヘテロ2量体構造をとるサイトカインの場合には注意を要する．たとえばIL-12 p40のKOマウスはIL-12に加えてIL-23を産生できないし，当初IL-12だけの欠損と考えられていたIL-12 p35 KOマウスはIL-35も産生できない．同様のことはサイトカイン受容体のKOマウスでも当てはまる．以下に，これまでに明らかにされているIL-12サイトカインファミリーの原虫感染における役割を示すが，サイトカインとその受容体のサブユニットの組合せを念頭においての理解が必要である．

1. IL-12

前述のように，IL-12はNK細胞やTh1によるIFN-γの産生やCD8陽性T細胞の活性化を誘導し，IFN-γによるマクロファージの活性化は細胞内寄生性原虫の排除にはたらく．マクロファージに寄生し，そのファゴリソソームの中で増殖するリーシュマニア原虫の排除には，このIL-12が決定的な役割を果たし[15,16]，IL-12投与が皮膚型に加えて内臓型リーシュマニア症にも奏効することが見出された[17,18]．病態のコントロールに内因性のIL-12が不可欠であることは，まずIL-12に対する中和抗体を投与する実験で示され[19]，次いでIL-12 p35 KOやIL-12 p40 KOマウスを用いた研究で示された[20]．IL-12 p35 KOに比べてIL-12 p40 KOマウスにおける原虫の増加がより大きいことより，IL-12に加えてIL-23もリーシュマニア原虫に対する感染防御に関与していることが示唆されている．

IL-12の重要性はマクロファージに選択的に寄生するリーシュマニア原虫に対してだけではなく，多様な細胞に感染する*T. gondii*や*T. cruzi*の感染においても示された[21,22]．また住血原虫であり細胞外で増殖する*Trypanosoma brucei brucei*や*Trypanosoma evansi*に対する感染防御においてもIL-12が不可欠であることが示された[23]．IFN-γ受容体KOマウスも両原虫に対して同様に感受性を示し，またIFN-γ KOマウスも*T. b. rhodesiense*に対して感受性となるなどの知見から，アフリカ睡眠病やナガナ病をひき起こす病原体に対してもIL-12はIFN-γの産生誘導を介して感染防御に機能していると考えられる．マラリアの場合，マラリア原虫は肝細胞の中で増殖する赤外型と赤血球の中で増殖する赤内型をとりうるが，いずれの場合もIL-12がIFN-γの産生誘導を介して感染防御に機能することが齧歯類に寄生するマラリア原虫を用いた研究から明らかにされた[24]．ただしマラリアにおいてIL-12/IFN-γは，原虫排除のみならず自己の組織破壊をもたらすこともあり，*Plasmodium berghei* ANKAによってひき起こされる脳炎や*Plasmodium berghei* NK65による肝炎はIL-12/IFN-γによってひき起こされることが知られている[25]．*Cryptosporidium parvum*は腸管上皮細胞に感染する細胞内寄生原虫であり，小児や免疫不全状態にある人に下痢をひき起こす日和見病原体である．この*Cryptosporidium*に対する感染防御機構の詳細はいまだに十分には理解されていないものの，IL-12/IFN-γの重要性については繰り返し報告されている[26,27]．

2. IL-23

原虫感染防御におけるIL-23の役割に関する報告は多くはないが，*T. gondii*の感染系において比較的研究が進んでいる．IL-23 p19 KOマウスは野生型マウスと同様のT細胞応答を示し，原虫数もうまくコントロールできるので，*Toxoplasma*の急性感染に対する防御にはIL-23は必須ではないようである[28]．ただし，IL-12 p40 KOマウスはIL-12 p35 KOマウスに比べて病態が重篤で，かつIL-12 p40 KOにリコンビナントIL-23を加えると病態がやや改善を示すことより，IL-12が存在しないような状況下ではIL-23が部分的に感染防御を補完すると考えられている．このときの防御はIFN-γ非依存的なメカニズムによると報告されている．

IL-23によって分化するTh17からは，IL-17をはじめとするサイトカインが産生される．原虫感染におけるIL-17の役割に関する報告は少ないが，KellyらはIL-17受容

体欠損マウスにおいて好中球の遊走が低下し，*T. gondii* に対する感染抵抗性が減弱することを報告している[29]．また，筆者らはIL-17欠損マウスにおいて炎症性サイトカイン産生低下を伴って *T. cruzi* 感染抵抗性が減弱することを見出している（未発表データ）．

3. IL-27

前述したように，IL-27には，これまでに免疫亢進と免疫抑制という2つの相反する作用が認められる．IL-27の役割は，とくにKOマウスを用いた原虫感染の実験系で明らかにされてきた[30]．

筆者らの作製したIL-27受容体α鎖（WSX-1）欠損マウスにおいては，*L. major* に対する感染抵抗性が野生型に比べて著しく低下していた[31]（図2a, b）．WSX-1欠損マウスでは，感染早期における所属リンパ節CD4陽性細胞のTh1への分化が障害されており，原虫抗原特異的IFN-γ産生も低下していた．興味深いことに，感染後期になると，IFN-γ産生は野生型と同程度にまで回復し，一部のWSX-1欠損マウスでは感染部位の腫脹の軽減も認められることから，*L. major* に対する防御免疫におけるIL-27の必要性は，感染早期に限定されるものと推察された．同様の結果がEBI-3欠損マウスについても報告されており[32]，*in vitro* の解析結果も併せて，IL-27/WSX-1が *L. major* 感染早期のTh1分化誘導に必須の役割を果たしていることが明らかにされた．

WSX-1欠損マウスは *T. cruzi* や *T. gondii* に対しても感染感受性を示したが，このときTh1分化の障害は認められず，むしろIFN-γを含むさまざまな炎症性サイトカインの過剰産生が生じ，肝細胞壊死に伴う肝機能障害などによって死亡していくことが示された（図2c, d）．IL-12やIFN-γを欠損するマウスでは，*T. cruzi* 感染時に原虫の排除能が低下し血中の原虫数は野生型に比べ著しく増

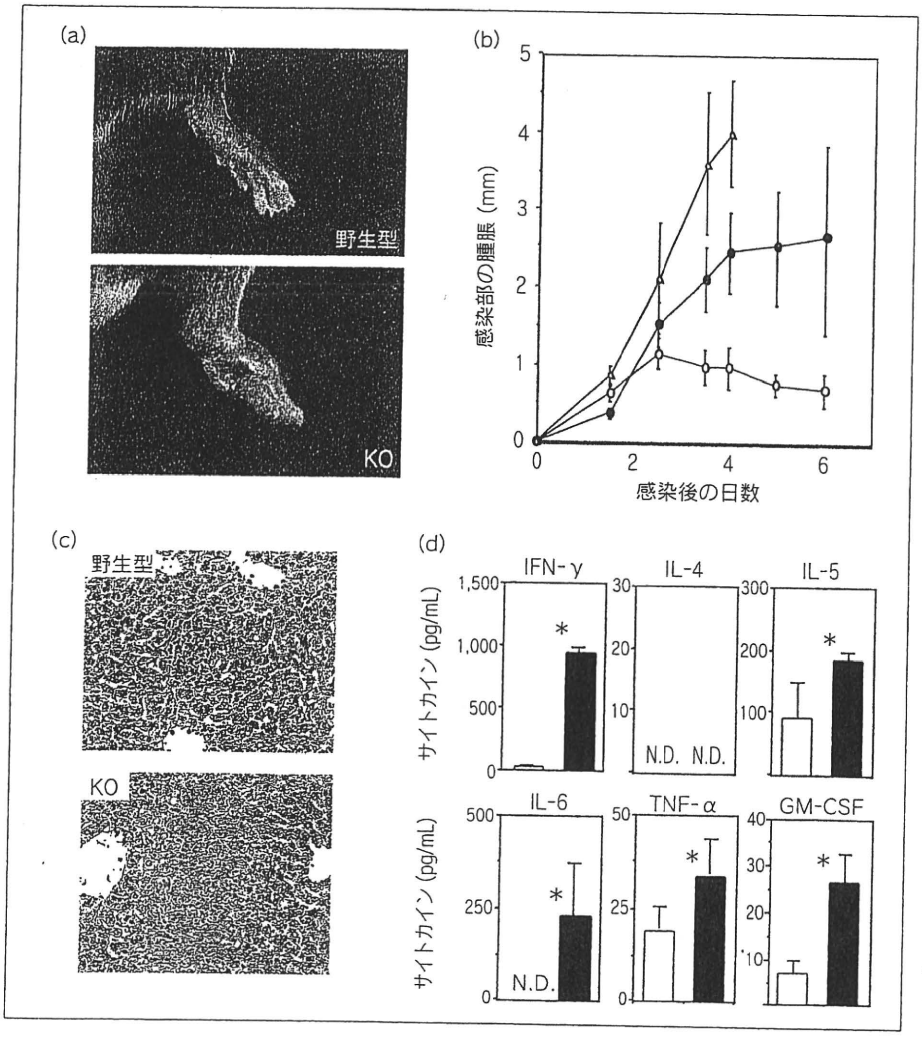

図2　原虫感染におけるIL-27の2つの役割

(a, b) WSX-1欠損マウスにおける *Leishmania major* 感染部位の腫脹．
(a) WSX-1欠損マウス(KO)は，Th1初期分化が障害されているため，*L. major* 感染抵抗性が減弱し，野生型に比べて著しい感染部位の腫脹をきたす．
(b) C57BL/6マウス(○)は分化したTh1により原虫を排除するが，BALB/cマウス(△)ではTh1分化障害のため原虫を排除できない．WSX-1欠損マウス（●）は，C57BL/6マウスの遺伝的背景をもつが，Th1分化異常のため原虫排除が障害されている．
(c, d) WSX-1欠損マウスにおけるサイトカインの過剰産生．
(c) *Trypanosoma cruzi* 感染時，WSX-1欠損マウス(KO)では肝臓の広範なネクローシス像が認められる．
(d) *T. cruzi* 感染後，WSX-1欠損マウスの血清中(■)には，野生型マウス(□)に比べ，さまざまな炎症性サイトカインの過剰産生が見られる．＊：$p < 0.05$ で有意差を認める．N. D.：検出限界以下．
（文献31，35より転載，一部改変）

加するが，肝細胞壊死はほとんど生じない．このことから，この肝障害は主としてIFN-γによってひき起こされており，IL-27にはIFN-γを含む炎症性サイトカインの産生を抑制することにより，感染に伴う過剰な炎症を抑制するはたらきがあることが明らかになった．IL-12の項で述べたように，感染時にTh1などによって産生されるIFN-γは，宿主にとって諸刃の剣であり，病原体を排除するとともに自らに致死的な炎症をひき起こしうる．IL-27はサイトカインの産生を抑制することにより，こうした過剰な炎症を制御していると考えられる．IL-27によるサイトカイン産生抑制の観点から，Artisらは，WSX-1欠損マウスにおける*L. major*に対する抵抗性の減弱は，感染初期の一過性のIL-4産生に対するIL-27による抑制作用が失われ，Th2分化が促進されたためという仮説を提示している[33]．

*T. gondii*感染では脳炎などの神経症状がひき起こされることがある．WSX-1欠損マウスで免疫抑制により*T. gondii*による慢性感染を誘導すると，マウスはTh17依存性のトキソプラズマ脳炎により死亡する．WSX-1欠損マウスでは，Th17に依存した実験的自己免疫性脳炎も増悪することから，IL-27にはTh17分化を抑制する作用があることも明らかになった．IL-27によるTh17分化抑制機構もIL-17産生制御を介して感染に伴う過剰な炎症の抑制にかかわっているものと考えられる．IL-27/WSX-1欠損マウスにおける原虫感染の解析結果を表1にまとめる．なお，ヒトの原虫感染症におけるIL-27の役割は明らかにされておらず，今後の研究が待たれる．

4. IL-35

原虫感染におけるIL-35の役割は明らかにされていない．前述のように，EBI-3欠損マウスにおけるTh1分化障害と*L. major*に対する抵抗性減弱が報告されているが[32]，この結果がIL-27とIL-35のどちらに依存したものかを明らかにするためには，p28単独欠損マウスやWSX-1欠損マウスとの詳細な比較，およびそれぞれのサイトカイン投与の結果などとの比較検討を必要とする．IL-35は，それ自体に免疫抑制作用があり，またTregを増殖させ，同時にTreg自体から産生されるとの報告があることなどから，Tregによる免疫抑制にかかわっていると推測されているが，その詳細は明らかではない．Tregからは，IL-10やTGF-βなどの免疫抑制にかかわる他のサイトカインも産生されるが，原虫感染におけるこれらのサイトカインの役割に関しては，すでに多くの報告があり，本稿ではその説明は割愛する．

おわりに

Th1/2という性質の異なるヘルパーT細胞サブセットの発見，およびTh1分化を誘導するIL-12の発見により，細胞内寄生性病原体に対する防御免疫におけるTh1/IL-12/IFN-γの重要性が広く認識されてきた．しかしながら，近年IL-12関連サイトカインが相次いで同定され，さらにTh17やTregなどの新しいCD4陽性細胞サブセットが同定され，ヘルパーT細胞の分化と，免疫制御におけるその役割の理解は新しい局面を迎えている（図3）．IL-12ファミリーサイトカインは，それぞれTh1分化誘導作用を

表1　IL-27/IL-27受容体欠損マウスの原虫感染における表現型

マウス(欠損する遺伝子)	病原体	Th反応	感染病態	文献
WSX-1$^{-/-}$	*Leishmania major*	初期Th1の低下	感染感受性の亢進 感染後期には正常なTh1	32
WSX-1$^{-/-}$	*Trypanosoma cruzi*	Th1，Th2，Th17の亢進	サイトカインの過剰産生による肝臓などの炎症の増悪	36
WSX-1$^{-/-}$	*Toxoplasma gondii* (急性)	IFN-γの過剰産生	IFN-γの過剰産生による肝臓などの炎症の増悪	37
TCCR$^{-/-}$ a)	*Leishmania donovani*	Th1の亢進	肝臓の炎症の増悪	38
WSX-1$^{-/-}$	*Toxoplasma gondii* (慢性，感染性脳炎)	Th17の亢進	感染性脳炎の増悪	9
EBI-3$^{-/-}$	*Leishmania major*	初期Th1の低下	感染感受性の亢進 感染後期には正常なTh1	33

a) TCCR（=WSX-1，IL-27受容体α鎖の別名）ノックアウトマウス[38]．

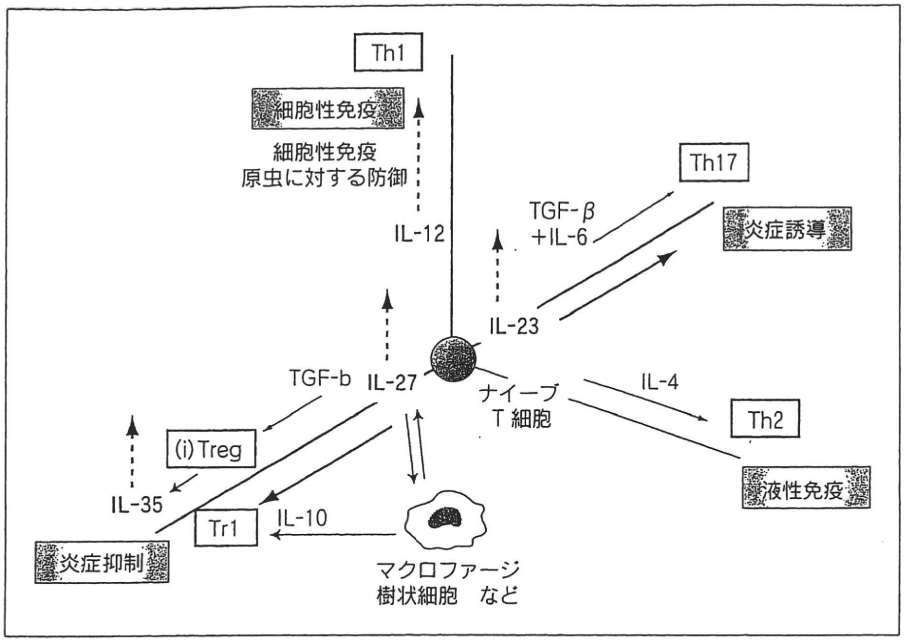

図 3　多元的なヘルパーT 細胞の分化と IL-12 サイトカインファミリーによる分化制御

Th1 と Th2 に加え，IL-23 により分化が促進される Th17 が同定された．IL-12 サイトカインファミリーは，Th1 分化誘導能をもつとともに，特異的な分化制御作用ももつ．IL-23 は，Th17 の分化誘導作用をもつ．IL-27 は Th17 の分化を抑制し，さらに T 細胞やマクロファージなどによる IL-10 産生を誘導する作用をもち，Tr1 とよばれる抑制性 T 細胞に類似した細胞集団への分化を促進すると考えられる．IL-35 は制御性 T 細胞（Treg，誘導型のものは iTreg とされる）から産生され，免疫抑制作用を示す．
太字は IL-12 サイトカインファミリーメンバーを示し，それぞれ Th1 分化誘導能を有している（破線矢印）．

もつとともに，免疫抑制や炎症誘導などの特異的な機能ももっており，感染免疫のみならず，免疫の関与するさまざまな疾患の病態生理において重要な役割を果たしている．

IL-12 サイトカインファミリーメンバーのうち，原虫に対する感染防御の観点から最も興味深いサイトカインは，IL-12 と IL-27 である．IL-12 は，直接 Th1 に作用し，IFN-γ 産生を誘導することから，原虫を含む細胞内寄生性病原体の排除において最も重用なサイトカインであると考えられ，実際，原虫感染における治療効果も確認されている．一方 IL-27 は，ナイーブ T 細胞が Th1 への分化を開始するうえで鍵となるサイトカインであり，原虫抗原で免疫する際に，Th1 型免疫を誘導するアジュバント*3 としての作用も認められる（未発表データ）．その一方で，IL-27 は，感染によりひき起こされる過剰な免疫・炎症を抑制する作用を有しており，組織損傷を防ぐことで，感染宿主を守るとともに，組織破壊に続発しうる自己免疫病態を抑制する作用をもっているものと考えられる．

IL-12 サイトカインファミリーメンバーは，相互にそのサブユニットを共有しており，それぞれのサブユニットの発現は，異なる転写制御を受けている[34]．今後，新たな組合せによる新しいサイトカインが同定され，それぞれのサイトカインについて知られていた機能が，別の（組合せによる）サイトカインの作用であることが判明する可能性もある．IL-12 サイトカインファミリーメンバーの解析がさらに進むことにより，感染防御免疫の新しい制御法が確立されることが期待される．

文　献

1) Harrington, L. E. *et al.*：*Nat. Immunol.*, 6, 1123-1132 (2005)
2) Park, H. *et al.*：*Nat. Immunol.*, 6, 1133-1141 (2005)
3) Oppmann, B. *et al.*：*Immunity*, 13, 715-725 (2000)
4) Pflanz, S. *et al.*：*Immunity*, 16, 779-790 (2002)
5) Collison, L. W. *et al.*：*Nature*, 450, 566-569 (2007)
6) Niedbala, W. *et al.*：*Eur. J. Immunol.*, 37, 3021-3029 (2007)
7) Trinchieri, G. *et al.*：*Prog. Growth Factor Res.*, 4, 355-368 (1992)
8) Takeda, A. *et al.*：*J. Immunol.*, 170, 4886-4890 (2003)
9) Stumhofer, J. S. *et al.*：*Nat. Immunol.*, 7, 937-945 (2006)
10) Batten, M. *et al.*：*Nat. Immunol.*, 7, 929-936 (2006)
11) Yoshimura, T. *et al.*：*J. Immunol.*, 177, 5377-5385 (2006)
12) Fitzgerald, D. C. *et al.*：*Nat. Immunol.*, 8, 1372-1379 (2007)
13) Awasthi, A. *et al.*：*Nat. Immunol.*, 8, 1380-1389 (2007)
14) Mosmann, T. R, Coffman, R. L.：*Annu. Rev. Immunol.*, 7, 145-173 (1989)
15) Reiner, S. L., Locksley, R. M.：*Annu. Rev. Immunol.*, 13, 151-177 (1995)
16) Heinzel, F. P. *et al.*：*J. Exp. Med.*, 177, 1505-1509 (1993)

*3　アジュバント：抗原やワクチンの免疫原性を高める目的で抗原とともに生体に投与される試薬類．免疫賦活剤，あるいは免疫増強剤の一種とも考えられる．

17) Murray, H. W., Hariprashad, J. : *J. Exp. Med.*, 181, 387-391 (1995)
18) Ghalib, H. W. *et al.* : *J. Immunol.*, 154, 4623-4629 (1995)
19) Heinzel, F. P. *et al.* : *J. Immunol.*, 155, 730-739 (1995)
20) Mattner, F. *et al.* : *Eur. J. Immunol.*, 26, 1553-1559 (1996)
21) Gazzinelli, R. T. *et al.* : *J. Immunol.*, 153, 2533-2543 (1994)
22) Aliberti, J. C. *et al.* : *Infect. Immun.*, 64, 1961-1967 (1996)
23) Barkhuizen, M. *et al.* : *J. Infect. Dis.*, 196, 1253-1260 (2007)
24) Sedegah, M. *et al.* : *Proc. Natl. Acad. Sci. USA*, 91, 10700-10702 (1994)
25) Yoshimoto ,T. *et al.* : *J. Immunol.*, 160, 5500-5505 (1998)
26) Chen, W. *et al.* : *Infect. Immun.*, 61, 3928-3932 (1993)
27) Urban, J. F., Jr. *et al.* : *J. Immunol.*, 156, 263-268 (1996)
28) Lieberman, L. A. *et al.* : *J. Immunol.*, 173, 1887-1893 (2004)
29) Kelly, M. N. *et al.* : *Infect. Immun.*, 73, 617-621 (2005)
30) Yoshida, H. *et al.* : *J. Biomed. Biotechnol.*, 2007, 79401 (2007)
31) Yoshida, H. *et al.* : *Immunity*, 15, 569-578 (2001)
32) Zahn, S. *et al.* : *Eur. J. Immunol.*, 35, 1106-1112 (2005)
33) Artis, D. *et al.* : *J. Immunol.*, 172, 4672-4675 (2004)
34) Goriely, S. *et al.* : *Nat. Rev. Immunol.*, 8, 81-86 (2008)
35) Hamano, S. *et al.* : *Immunity*, 19, 657-667 (2003)
36) Villarino, A. *et al.* : *Immunity*, 19, 645-655 (2003)
37) Rosas, L. E. *et al.* : *Am. J. Pathol.*, 168, 158-169 (2006)
38) Chen, Q. *et al.* : *Nature*, 407, 916-920 (2000)